Sedimentology of the mid-Carboniferous fill of the Olta paleovalley, eastern Paganzo Basin, Argentina: Implications for glaciatio....

Article *in* Journal of South American Earth Sciences · March 2018

DOI: 10.1016/j.jsames.2018.03.015

CITATIONS
0

READS
170

5 authors, including:

John L Isbell
University of Wisconsin - Milwaukee
128 PUBLICATIONS **2,369** CITATIONS
SEE PROFILE

Kathryn Pauls
University of Wisconsin - Milwaukee
16 PUBLICATIONS **3** CITATIONS
SEE PROFILE

Carlos Oscar Limarino
University of Buenos Aires
207 PUBLICATIONS **2,651** CITATIONS
SEE PROFILE

Laura Jazmín Schencman
University of Buenos Aires
11 PUBLICATIONS **6** CITATIONS
SEE PROFILE

Journal of South American Earth Sciences 84 (2018) 127–148

Contents lists available at ScienceDirect

Journal of South American Earth Sciences

journal homepage: www.elsevier.com/locate/jsames

Sedimentology of the mid-Carboniferous fill of the Olta paleovalley, eastern Paganzo Basin, Argentina: Implications for glaciation and controls on diachronous deglaciation in western Gondwana during the late Paleozoic Ice Age

Levi D. Moxness[a,1], John L. Isbell[a,*], Kathryn N. Pauls[a], Carlos O. Limarino[b,c], Jazmin Schencman[b]

[a] Department of Geosciences, University of Wisconsin-Milwaukee, 3209 N. Maryland Ave., Milwaukee, WI, 53211, USA
[b] Departamento de Ciencias Geológicas, Universidad de Buenos Aires, IGeBA, Ciudad Universitaria, Pabellón II, 1428, Buenos Aires, Argentina
[c] Consejo Nacional de Investigaciones Científicas y Técnicas (CONICET), Sarmiento 440, Buenos Aires, Argentina

ARTICLE INFO

Keywords:
Late Paleozoic Ice Age
Paleoclimate
Pennsylvanian
Paleovalley
Gondwana
Glaciation
Argentina

ABSTRACT

Both global and regional climate drivers contributed to glaciation during the late Paleozoic Ice Age (LPIA). However, the transition from icehouse to greenhouse conditions was asynchronous across Gondwana suggesting that, in some cases, regional controls played a significant role in deglaciation. Of particular interest to understanding changing LPIA climatic conditions, is the eastern Paganzo Basin. This region was flanked by ice centers in the Precordilleran and Sierras Pampeanas regions of Argentina on the west, and major ice sheets in the Paraná, Chaco-Paraná, and Sauce Grande basins to the east, all of which resided between ~40 and 65° S latitude. Hypotheses on the occurrence of ice in the eastern Paganzo Basin are based on interpretations of the narrow, steep-walled, Olta-Malanzán paleovalley as carved by an alpine glacier or by an outlet glacier draining an eastern ice sheet, and that glaciers deposited coarse clastics within the paleovalley. However, we found no evidence for glaciation. Rather, gravel from prograding alluvial fans/fan deltas and rock falls ponded drainage resulting in lacustrine activity in the eastern end of the valley. A transition from either subaerially or shallow subaqueously deposited sandstones to marine mudstones in the western end of the Olta paleovalley suggest a marine transgression, which, in turn, was overlain by deposits of prograding Gilbert-type deltas. Dropstones were from rock falls off valley walls and rafting by lake ice rather than from icebergs. Therefore, we conclude that the climate in western Argentina resulted from uplift induced glaciation in the Precordilleran region and along the western margin of the Paganzo Basin, and the occurrence of a precipitation shadow to the east. The disappearance of the western glaciers during the mid-Carboniferous, prior to deglaciation elsewhere at the same paleolatitude, resulted from a westward shift in the position of the active margin, collapse of the glaciated upland(s), and an expansion of the precipitation shadow across the whole of western Argentina.

1. Introduction

The Late Paleozoic Ice Age (LPIA; ~372 to 259 Ma) represents the longest glacial interval during the last 541 Myr. Recent studies suggest that this event was characterized by multiple, glacial and non-glacial intervals each lasting up to 10 Myr with individual glaciations marked by numerous ice sheets that waxed and waned diachronously across the supercontinent (López-Gamundí, 1997; Isbell et al., 2003, 2012; Fielding et al., 2008a, 2008b; Montañez and Poulsen, 2013; Frank et al., 2015). Glaciation began in northern Gondwana and other scattered sites in the late Devonian with the main phase of the LPIA commencing in western and northern South America in the Mississippian (Viséan) before ice sheets spread across Gondwana in the Late Mississippian, Pennsylvanian and Early Permian (Caputo and Crowell, 1985; López-Gamundí, 1997; Isbell et al., 2003, 2012; Fielding et al., 2008b; Limarino et al., 2014). The transition out of the LPIA into greenhouse/hothouse conditions was diachronous, beginning first in western South America in the Early Pennsylvanian and ending in eastern Australia

* Corresponding author. Department of Geosciences, University of Wisconsin-Milwaukee, Rm. 366 Lapham Hall, 3209 N. Maryland Ave., Milwaukee Wi 53211, USA.
E-mail addresses: ldmoxness@gmail.com (L.D. Moxness), jisbell@uwm.edu (J.L. Isbell), kpauls@uwm.edu (K.N. Pauls), oscarlimarino@gmail.com (C.O. Limarino), jazminsch@gmail.com (J. Schencman).
[1] Current address: North Dakota Geological Survey, 600 East Boulevard, Dept. 405, Bismarck, ND 58505-0840.

https://doi.org/10.1016/j.jsames.2018.03.015
Received 30 November 2017; Received in revised form 11 March 2018; Accepted 22 March 2018
Available online 24 March 2018
0895-9811/

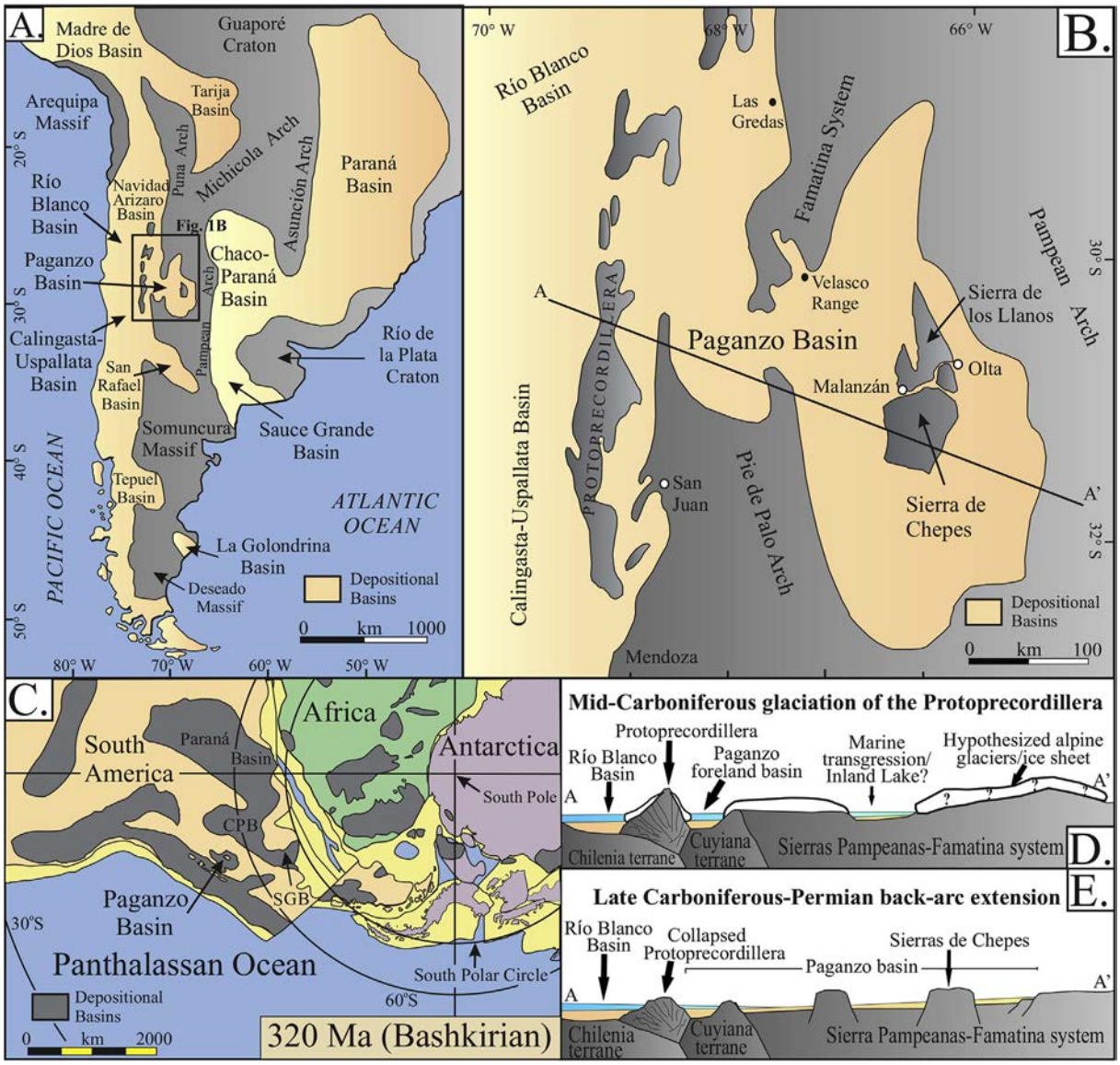

Fig. 1. (A) Late Paleozoic basins (yellow) and surrounding uplands (gray) of southern South America. (B) Paganzo Basin location map. (C) Paleogeographic reconstruction of western Gondwana showing depositional basins and the location of the Paganzo, Paraná, Chaco-Paraná (CPB), and Sauce Grande (SGB) basin in southern South America (modified from Lawver et al., 2011). D and E) schematic reconstructions (A-A′) of the Paganzo basin and its position east of the Protoprecordillera, a fold-thrust belt that housed glaciers in the mid-Carboniferous prior to its extensional collapse through the Pennsylvanian (modified after Limarino et al., 2006). D shows hypothetical location of glaciers (modified after Astini et al., 2009) in what would become the eastern Paganzo Basin that is tested in this paper. (For interpretation of the references to color in this figure legend, the reader is referred to the Web version of this article.)

during the early Late Permian (Caputo and Crowell, 1985; Veevers and Powell, 1987; Fielding et al., 2008c; Frank et al., 2015). Although many aspects of the LPIA remain controversial (cf. Horton and Poulsen, 2009; Montañez and Poulsen, 2013), resolving the timing and extent of the waxing, waning, and disappearance of ice centers across Gondwana is of particular interest for developing an understanding of the drivers of long-term global and regional climate change.

Basins in western Argentina (e.g., Calingasta-Uspallata, Rio Blanco, and western Paganzo basins; Fig. 1) record the onset of the Viséan stage of glaciation, and were some of the first in Gondwana to be deglaciated during the Early Pennsylvanian (cf. López-Gamundí et al., 1994; López-Gamundí, 1997; Caputo et al., 2008; Henry et al., 2008). However, basins in east-central South America (e.g., Paraná, Chaco-Paraná, and Sauce Grande basins; Fig. 1) experienced the glacial to post-glacial transition later during the Late Pennsylvanian and Early Permian (cf. López-Gamundí et al., 1994; Holz et al., 2008; Rocha Campos et al., 2008; Limarino et al., 2014; Cagliari et al., 2016; Griffis et al., 2017) despite their location at essentially the same paleolatitude (between ~40 and 65° S latitude) as the western Argentine basins (Fig. 1C; Powell and Li, 1994, Isbell et al., 2012; Lawver et al., 2011; Torsvik and Cocks, 2013). Of particular interest to the paleoclimate history of South America and Gondwana is the eastern Paganzo Basin and the Olta-Malanzán paleovalley (Figs. 1 and 2). Although these features were located between the eastern and western glaciated basins of South America (Fig. 1), the presence and extent of ice there is highly controversial. Several authors suggest that the eastern Paganzo Basin was the site of either valley glaciers on uplands or an extensive ice sheet that drained westward as an outlet glacier through the Olta-Malanzán paleovalley (Fig. 1D; cf. Sterren and Martínez, 1996; Aquino et al., 2014; Enkelmann et al., 2014; Socha et al., 2014); however, others suggest that limited or no ice occurred in this region (cf. Andreis et al., 1986).

One of the central postulates for the existence of Carboniferous glaciers in the easternmost part of the Paganzo Basin is based on interpretations of the Malanzán Fm. (Fig. 3) as glacigenic in origin

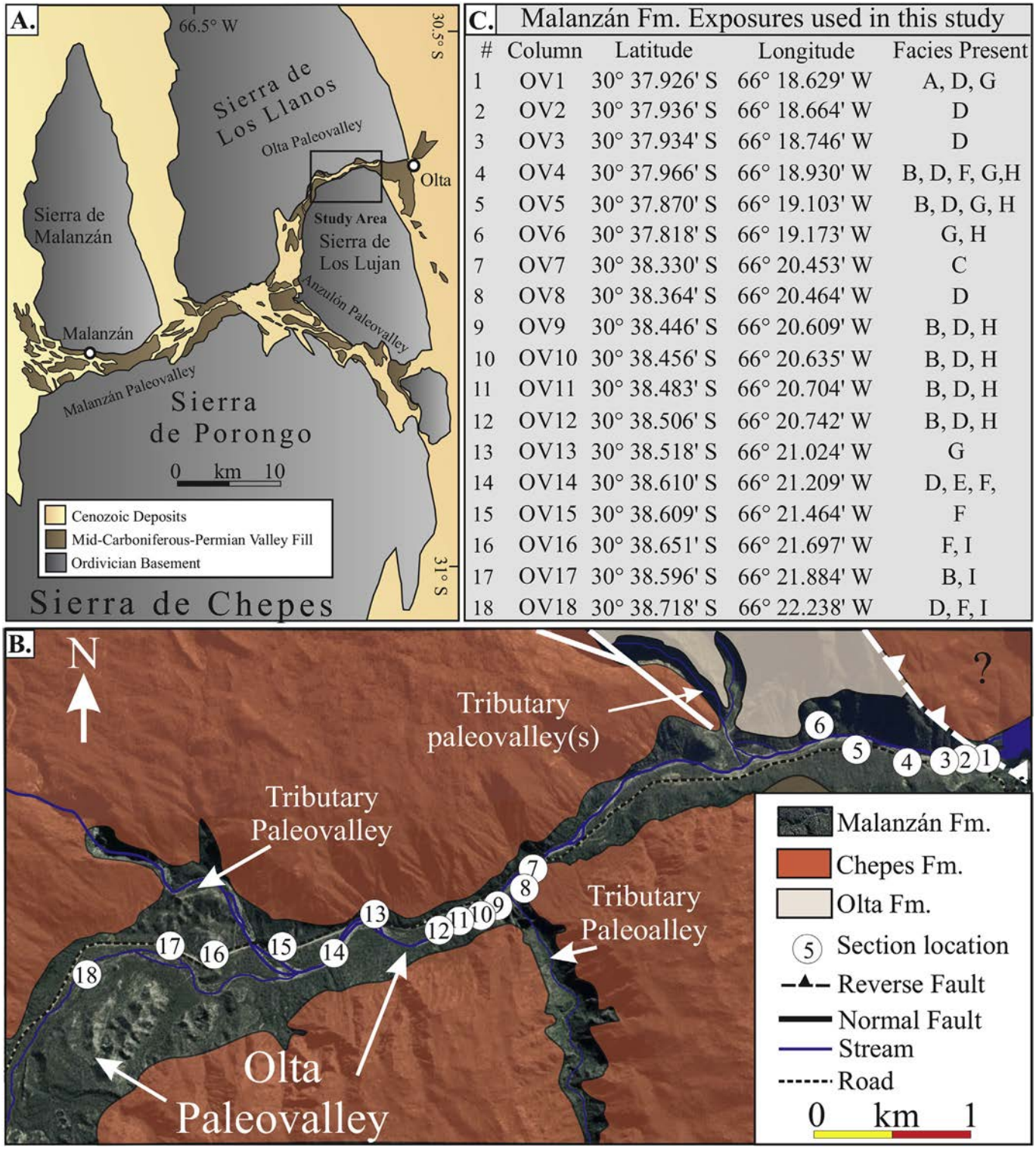

C. Malanzán Fm. Exposures used in this study

#	Column	Latitude	Longitude	Facies Present
1	OV1	30° 37.926' S	66° 18.629' W	A, D, G
2	OV2	30° 37.936' S	66° 18.664' W	D
3	OV3	30° 37.934' S	66° 18.746' W	D
4	OV4	30° 37.966' S	66° 18.930' W	B, D, F, G,H
5	OV5	30° 37.870' S	66° 19.103' W	B, D, G, H
6	OV6	30° 37.818' S	66° 19.173' W	G, H
7	OV7	30° 38.330' S	66° 20.453' W	C
8	OV8	30° 38.364' S	66° 20.464' W	D
9	OV9	30° 38.446' S	66° 20.609' W	B, D, H
10	OV10	30° 38.456' S	66° 20.635' W	B, D, H
11	OV11	30° 38.483' S	66° 20.704' W	B, D, H
12	OV12	30° 38.506' S	66° 20.742' W	B, D, H
13	OV13	30° 38.518' S	66° 21.024' W	G
14	OV14	30° 38.610' S	66° 21.209' W	D, E, F,
15	OV15	30° 38.609' S	66° 21.464' W	F
16	OV16	30° 38.651' S	66° 21.697' W	F, I
17	OV17	30° 38.596' S	66° 21.884' W	B, I
18	OV18	30° 38.718' S	66° 22.238' W	D, F, I

Fig. 2. (A) Simplified geologic map of the Olta-Malanzán paleovalley and surrounding ranges (modified from Net and Limarino, 1999). (B) Location map of study sections Google Earth satellite image of the Olta paleovalley showing the geology (modified after Sterren and Martínez, 1996) and locations of measured stratigraphic columns. (C) Stratigraphic sections, locations and major facies contained in the measured sections in this study.

(Sterren and Martínez, 1996; Astini, 2010; Enkelmann et al., 2014; Rabassa et al., 2014; Socha et al., 2014). Due to the paleoenvironmental, paleogeographic, and paleoclimatological importance of the Malanzán Fm. and the ambiguity that surrounds the origin of these deposits, further investigation is warranted. Here, we report on the depositional setting of the Malanzán Fm. in the Olta paleovalley to resolve the size, timing, and extent of glaciers in South America, to resolve the glacial history of the eastern Paganzo basin, and to understand reasons for diachronous deglaciation during the LPIA. Fieldwork was conducted in 3/2015 and 8/2016. We employed standard stratigraphic and sedimentological techniques to examine and measure 18 stratigraphic sections of the Malanzán Fm. (Figs. 2 and 4). Poorly sorted clastic rocks were identified using the classification scheme of Hambrey and Glasser (2012).

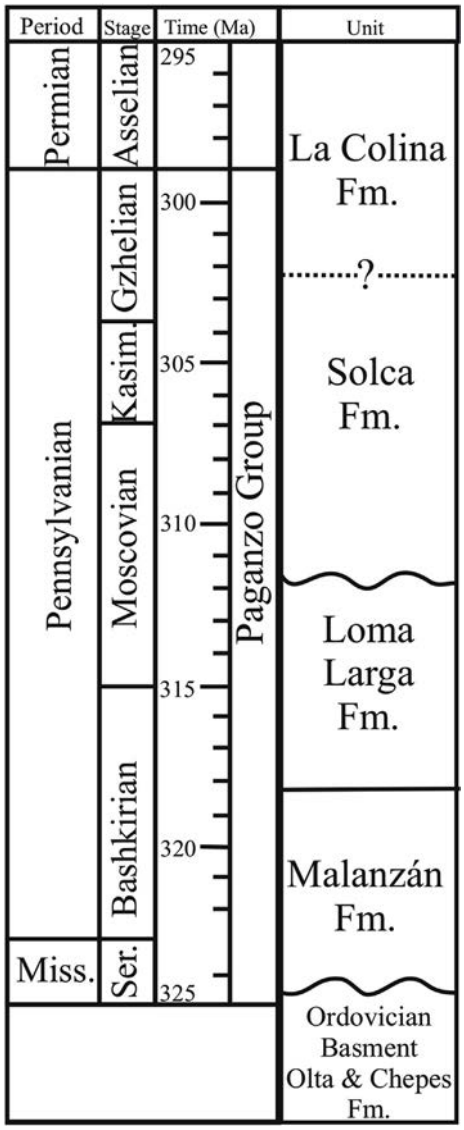

Fig. 3. Stratigraphic chart for the Late Paleozoic units of the Olta-Malanzán paleovalley (modified from Gutiérrez and Limarino, 2001; Gulbranson et al., 2010). Ages are extrapolated from radiogenic dates of coeval deposits in the western Paganzo basin (Gulbranson et al., 2015).

1.1. Geologic setting and objectives

One of the earliest lines of evidence for glaciation (Viséan to early Bashkirian) associated with the main phase of the LPIA is recognized from the Precordillera region in western Argentina. The Protoprecordillera (Fig. 1), also referred to as the Tontal Arch, was an ancient uplift, which coincided with the present position of the Precordillera mountain range. This upland was interpreted by some to have developed as a fold thrust belt during late stages of the Chañic Orogeny (Late Devonian to Mississippian) as the Chilenia terrane accreted to the western margin of Gondwana (e.g., Ramos et al., 1984, 1986; Limarino et al., 2006, 2014, Fig. 1D). In this belt, glacigenic deposits occur in deeply-incised paleovalleys > 1000 m deep that are oriented sub-radially away from the uplift and directed into the adjacent Calingasta-Uspallata, Rio Blanco, and western Paganzo basins (Fig. 1B; cf. López-Gamundí et al., 1994; López-Gamundí and Martinez, 2000; Dykstra et al., 2006; Henry et al., 2008). Serpukhovian-Bashkirian glaciers were also associated with the Sierras Pampeanas ranges in the central to western portion of the Paganzo Basin (Limarino and Gutiérrez, 1990; Limarino et al., 2002, 2014; Marenssi et al., 2005; Henry et al., 2008; Astini, 2010). Glaciers disappeared in these regions during the Early Pennsylvanian, possibly associated with the collapse of the upland during the Pennsylvanian and Permian as the active margin of Gondwana shifted to the west, and the region, including a developing Paganzo Basin, underwent back-arc extension (Fig. 1E; Ramos, 1988; López-Gamundí et al., 1994; Limarino et al., 2002, 2006, 2014; Isbell et al., 2012). However, Astini et al. (2009) and Astini (2010) envisioned a different Carboniferous history that started with widespread regional uplift for western Argentina and erosion of an extensive peneplain that developed due to the occurrence of erosion beneath an extensive ice cap across much of the region ~325–340 Ma (Fig. 1D). This was then followed by back-arc extension and associated glacial contraction to remnant ice centers located on uplifted blocks that developed in and around the Paganzo Basin ~305-325 Ma. Under this scenario, these glaciers cut a series of valleys into and across these uplifted blocks as the ice sheet collapsed. This tectonic regime is hypothesized to have been the result of rollback of a descending slab during the docking of the Chilenia Terrane, which was followed by inversion of the area into a retroarc foreland basin as renewed subduction shifted farther west during the latest Carboniferous and Early Permian.

The major basement uplifts within and along the margins of the Paganzo Basin today are inferred to have been topographic highs during the late Paleozoic (Jordan et al., 1989; López-Gamundí et al., 1994; Limarino and Spalletti, 2006; Enkelmann et al., 2014), They are noteworthy for their potential to have hosted glaciers during the LPIA. One block, containing the present-day Sierra de Los Llanos, the Sierra de Lujan, the Sierra de Malanzán, the Sierra del Porongo, and the Sierras de Chepes (Figs. 1 and 2), lies within the Paganzo basin nearly 250 km to the east of the Precordillera region. These ranges are composed primarily of Ordovician granite (Chepes Fm.) and schist (Olta Fm.). Cut into these basement blocks, is a narrow valley system, the Olta and Malanzán valleys (Figs. 2B and 5) that are superimposed on, and exhuming Carboniferous and Permian deposits of the Olta-Malanzán paleovalley. The Anzulón paleovalley (Fig. 2A) was also part of this system, but it does not expose strata that are of interest for this study. In plan view, the Olta-Malanzán valley displays a “lazy S” shape (Fig. 2A). The main axis of the paleovalley stretches approximately 40 km and narrows from its width of ~5500 m in the west (village of Malanzán) to less than 500 m on the eastern end of the valley near the city of Olta (Fig. 2). In several places, the paleovalley is less than 200 m wide, especially where a small modern tributary valley enter the Olta valley (near section OV8; Fig. 2B). Tributary are also cutting into Carboniferous deposits and are exhuming small tributary paleovalleys that entered the main paleovalley (Fig. 2B). This Olta-Malanzán paleovalley system has alternately been interpreted to be either glacially carved (cf. Sterren and Martínez, 1996; Enkelmann et al., 2014; Rabassa et al., 2014; Socha et al., 2014) or tectonically formed as a fault-bounded depression (Andreis et al., 1986; Buatois and Mángano, 1995; Net and Limarino, 1999).

Late Paleozoic deposits preserved in the valley are represented by at least four formations belonging to the Paganzo Group (Fig. 3). The basal fill is the Malanzán Fm., which is described in detail from exposed strata in the western Malanzán portion of the paleovalley (Azcuy, 1975; Andreis et al., 1986; Azcuy et al., 1987; Buatois and Mángano, 1995), but which also includes the basal fill of the valley to the east near Olta (Bracaccini, 1948; Sterren and Martínez, 1996; Gutiérrez and Limarino, 2001; Net et al., 2002). Palynological assemblages are used to correlate the Malanzán Fm. with the Middle Carboniferous (Late Serpukhovian to Bashkirian) lower Paganzo Group in western portions of the Paganzo basin (Gutiérrez and Limarino, 2001; Pérez Loinaze, 2009; Gulbranson et al., 2010; Césari et al., 2011). The Malanzán Fm. directly overlies basement and contains abundant conglomerates, breccias, and scattered diamictites, which interfinger laterally and intercalate vertically with graded and cross-laminated sandstones and mudstones (Andreis et al., 1986). The origin of these strata is problematic as they are interpreted either as glacial deposits (Sterren and Martínez, 1996;

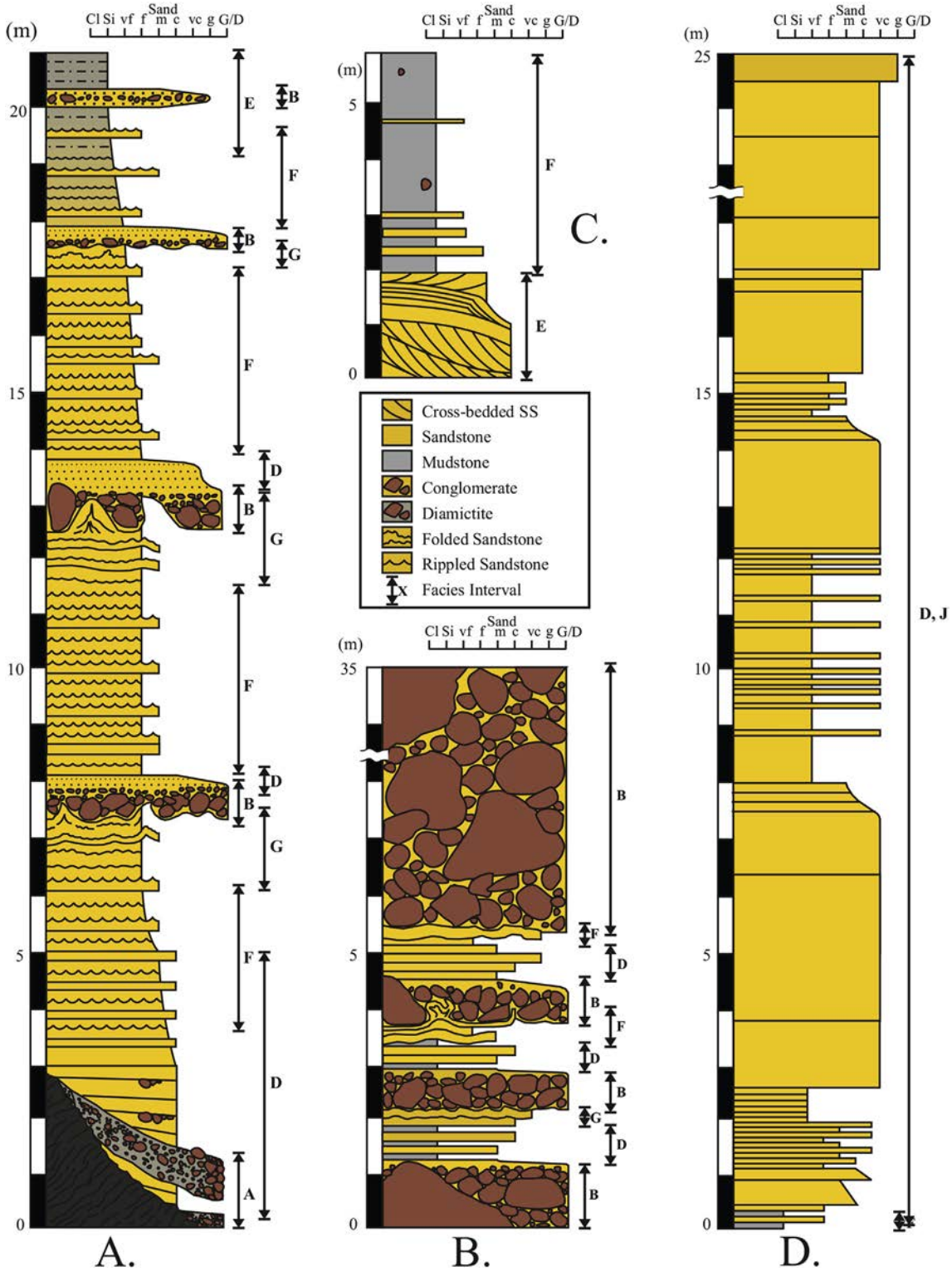

Fig. 4. Generalized and simplified stratigraphic columns displaying the facies identified in this study. Column A represents a composite of the lowermost eastern sections (OV1-6; Table 1; Fig. 1). Column B represents a composite of coarse-grained strata in the middle of the valley (OV9-12). In the western portion of the study area, column C represents part of the fining-upward succession (OV14) and column D the uppermost coarsening-upward succession (OV15-18).

Enkelmann et al., 2014; Rabassa et al., 2014; Socha et al., 2014), or sediment gravity flows on alluvial fans, and/or lacustrine/marine deposits (Andreis et al., 1986; Buatois and Mángano, 1995; Gutiérrez and Limarino, 2001). Drainage in the Olta-Malanzán paleovalley is interpreted to have flowed towards the west (Andreis et al., 1986; Sterren and Martínez, 1996). Later Carboniferous and Permian boulder-bearing diamictites and conglomerates, paleosols, medium- and coarse-grained sandstones and fine-grained sandstones displaying m-scale trough cross-bed sets occur in the overlying Loma Larga, Solca, and La Colina formations (Fig. 3), which are interpreted as having been deposited by braided-fluvial, alluvial fan, and possibly eolian processes suggesting possible increasing aridification in the basin through time (Andreis

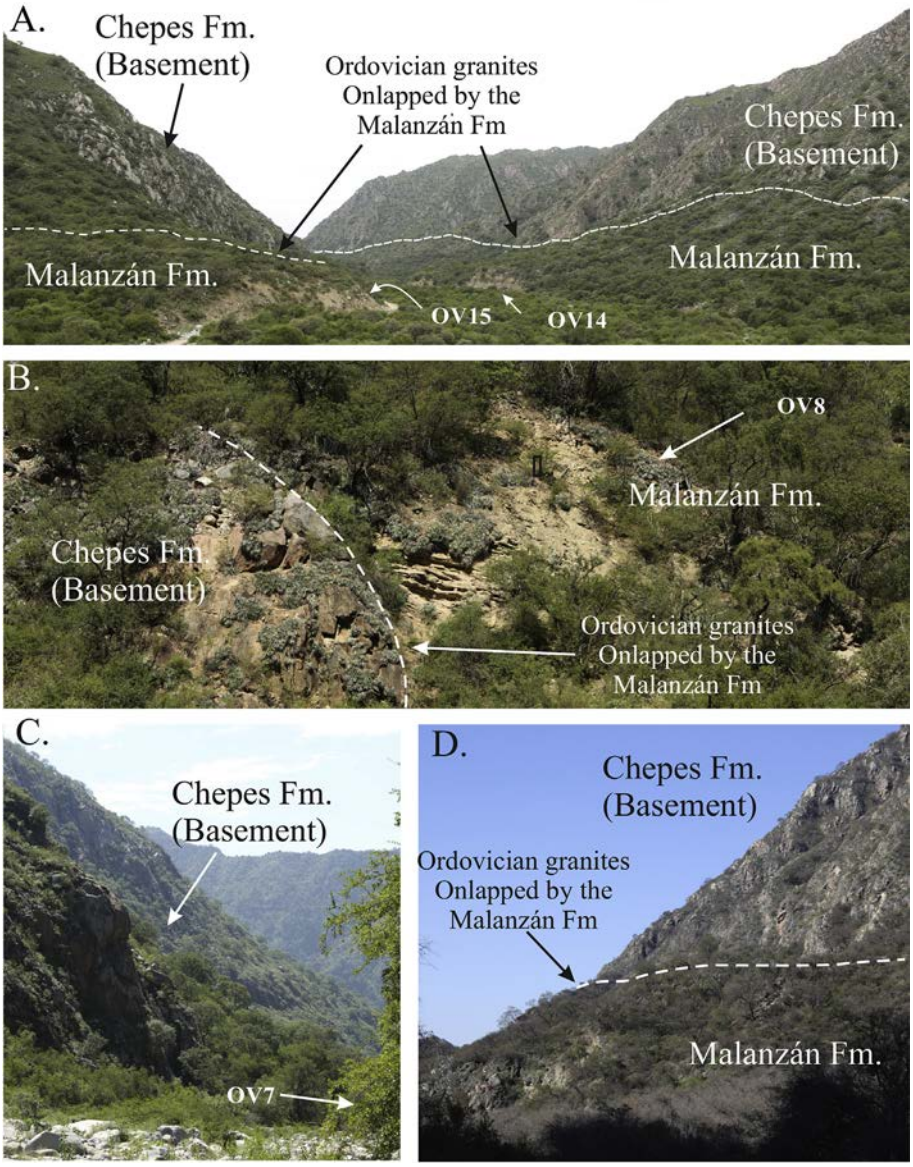

Fig. 5. Photos showing the onlapping relationship between deposits of the Malanzán Fm. and Ordovician basement rocks. (A) View looking east from section OV16. (B) View of section OV8 showing onlapping of sandstone onto steeply dipping granitic basement. (C) View looking east from section OV7 showing a near vertical wall of Granite along the northern valley wall. (D) View looking east at the southern valley wall from near section OV9.

et al., 1986; Gulbranson et al., 2015). Here we focus on the Malanzán Fm. in the Olta portion of the paleovalley system to determine its origin and climatic significance.

2. Lithofacies analysis

Outcrops of the Malanzán Fm. are exposed by modern incision of the Río Olta, which flows eastward through the study area. Stratigraphically, the lowest strata occur in the eastern end of the valley while the western end of the valley tends to expose higher stratigraphic units. Strata of the Malanzán Fm. in the Olta paleovalley are composed of 9 lithofacies (Table 1; Fig. 4) and described below. Although the base of the Malanzán Fm. rests on basement rocks, the contact was observed directly only in sections OV1, OV8, and near OV13 (Figs. 2 and 4) where strata lap onto the underlying basement along a high relief nonconformity (Figs. 5 and 6). At OV1, the unconformity is cut on schist and dips at 15 to 20° to the WNW. Here the bedrock surface is jagged and uneven, with thin slabs of schist that project into the overlying diamictite (Fig. 6A and B). Throughout the paleovalley, strata of the Malanzán Fm. abuts against walls of granite that slope from 30 to 80° (Figs. 5 and 6C). No striations, grooves, or polished surfaces were observed on the basement unconformity. The overall facies trends are characterized by basal clast-rich sandy diamictite and horizontally-and cross-laminated coarse sandstones overlying basement in the eastern-most sections (OV1-OV3; Figs. 2 and 4A), fining upwards to ripple cross-laminated fine and medium-grained sandstones, which are folded beneath intercalated beds of sandy conglomerate (OV5-OV4) and continue to fine upwards until the succession is dominated by laminated mudstone. Outcrops in the central portion of the valley near the steep paleovalley walls contain boulder breccias (OV7), and horizontally laminated sandstones (OV8), but nearby tributary paleovalley sections are dominated by interbedded boulder conglomerates and rare diamictites that interfinger laterally with folded sandstone and mudstone (OV9-OV12; Figs. 2 and 4B). The uppermost sections in the western portion of the study area show a fining upward succession (OV14; Figs. 2 and 4C) that is then overlain by a coarsening-upwards trend from laminated mudstones to sandy/gravely clinoforms (OV15-OV18; Figs. 2 and 4D).

Table 1
Facies description and interpretations for the Malanzán Formation in the Olta paleovalley, Argentina.

Lithofacies	Lithologies	Distinctive features	Bed thickness	Interpretation
A Clast-rich sandy diamictite	Massive, matrix- to clast-supported diamictite with a muddy sand matrix	Body consisting of clast-supported nose and matrix-supported tail with boulders protruding through unit top	0–1.4 m	Debris flows on fan surfaces and into lake near moderately sloped valley walls
B Sandy conglomerate	Massive to graded, matrix to clast-supported cobble-rich conglomerate with a sand matrix	Horizontal laminations, grading	0.2–32.7 m	Alluvial fan/fan delta
C Boulder breccia	Massive, clast-supported breccia with sandstone and mudstone between angular boulders	Heavily deformed sandstone and mudstone beds between boulders	8.2 m	Direct rockfall into lake near steep valley walls
D Graded sandstone	Massive or graded gravelly coarse-grained sandstone to ripple cross-laminated fine sandstone with thin silt drapes	Horizontal laminations, asymmetrical ripples, ripple cross-laminations, outsized clasts, dewatering structures, prod marks, and load/flames	0.1–0.6 m	Turbidity current/hyperpycnal flow-dominated deposition in shallow lake settings
E Medium to coarse-grained cross-bedded sandstone	Medium- to coarse-grained, trough, cross-bedded sandstone		0.1–0.5 m	Progradation and aggradation of a channelized fluvial system, a fan-delta lobe or a delta-mouth bar.
F Laminated mudstone	Thin horizontal laminations of mud with minor very fine sand and occasional outsized clasts	Outsized pebbles and cobbles	0.1–8.1 m	Suspension settling in distal lake settings with outsized clasts rafted by lake ice or vegetation
G Symmetrically rippled and bedded sandstone	Thin to very thin beds of symmetrically-rippled fine- to medium- to grained Ss, often overlain by horizontally-laminated siltstone	Symmetrical ripples, outsized clasts, unidirectional ripple cross-lamination	0.1–0.2 m	Wind-driven wave action in areas of the lake above wave-base level reworking sands of Facies D
H Folded sandstone and mudstone	Coherent folded beds of sandstone and mudstone up to 1.5 m in thickness	Load/flame structures, convolute bedding, truncated beds	0.2–1.5 m	Rapid loading of Facies D and E by cobble- and boulder-rich debris flows of Facies B. Seismic action and liquefaction possible
I Sandy to gravely clinoform	Massive to graded coarse- to fine-grained sandstone	Large-scale foreset and bottomset beds	0.1–2.3 m	Hyperpycnal flow of Gilbert-type delta progradation into freshwater

2.1. Facies A: clast-rich sandy diamictites

2.1.1. Facies A: clast-rich sandy diamictites description

Clast-rich, sandy diamictite occurs in sections OV1, OV9, and OV10 (Fig. 2) and consists of clast rich, intermediate to sandy (> 10% mud), massive diamictite. At OV1, diamictite rest on underlying schistose basement rocks, or is separated from the basement by < 1 m of horizontally laminated or bedded, pebble-bearing, coarse-grained sandstone, all of which onlap the basement (Fig. 7). The diamictite is wedge-shaped in cross-section (Fig. 7A) with one end of the unit ending as a clast-supported diamictite in a rounded, “nose-like” margin (Fig. 7B and D), while the opposite margin ends as a matrix-supported diamictite that onlaps the basement. Maximum unit thickness is 1.5 m near the “nose” of the unit and thins and pinches out where the unit onlaps basement. The facies predominantly contain subrounded pebbles and cobbles in a muddy, sand-rich matrix. However, an accumulation of subangular clast-supported boulders up to 60 cm in diameter (long-axis) defines the “nose” of the body (Fig. 7B and C). Clasts are mostly granitic with minor schist and quartzite clasts, and the clasts show no clear faceted, polished, striated sides, or preferred orientations. This facies displays sharp and erosional lower contacts and sharp upper contacts with boulders protruding from the top of the unit (Fig. 7A and C). Adjacent to the steeply dipping “nose,” gravelly stringers of sandstone (Facies D) onlap the diamictite. Laterally, these sands fine and thin away from the diamictite body (Fig. 7B and D).

In section OV9 and OV10 (Fig. 2), clast-rich, sandy diamictites are part of a thick body of sandy conglomerates (Facies B) that emanates from a tributary paleovalley. These diamictites and conglomerates downlap, interfinger with, cut into, and grade vertically and laterally into pebble to boulder conglomerates (Facies B), graded sandstones (Facies D) and symmetrically rippled sandstones (Facies G) within the main paleovalley (Fig. 7E). These diamictites are up to 2.5 m thick, massive to inversely graded, and have half a meter to meter-scale boulders protruding from the top of the deposit. In some places, the diamictites cut and/or are loaded into the underlying sandstone, with sandstone flame structures occurring along the margins of the diamictites and extending upward as much as 60 cm into the overlying diamictite unit. In some cases, the flame structures pierce and are extruded through overlying beds.

2.1.2. Facies A: clast-rich sandy diamictites interpretation

Differentiation of glacial diamictites from nonglacial mass-transport deposits is problematic (Visser, 1983), but at section OV1, the diamictite has several features similar to cohesive subaqueous debris flows. These flows commonly develop a frontal concentration of large clasts resulting in a clast-supported snout and a matrix-supported tail, “floating” boulders and cobbles that protrude through the top of the deposit, and out-runner clasts carried beyond the nose of the bed by associated turbidity currents (Postma et al., 1988; Mulder and Alexander, 2001; Sohn, 2000; Talling et al., 2012).

Resedimented glacial diamictites are reported from paleovalleys in the western Paganzo basin (Kneller et al., 2004; Dykstra et al., 2006; Henry et al., 2008; Limarino et al., 2014), but are associated with striated surfaces, true subglacial tillites, and faceted and striated clasts. The absence of these features in the Olta paleovalley suggests a non-glacial source for the remobilized sediment. Evidence of mass transport deposits are common in steep-walled mountain valleys (Van Steijn, 1996; Godt and Coe, 2007). This facies is interpreted to be deposited by debris flows off the valley walls into a standing body of water that occupied the central portion of the paleovalley. Diamictites associated with sandy conglomerates (Facies B; section OV9, OV10) also have characteristics similar to debris flow deposits (e.g. clast protruding from the top of the flow, massive and inverse grading; cf. Sohn, 2000). These diamictites were likely the result of deposition on alluvial fans/fan deltas where they flowed out of tributary valleys into the main Olta paleovalley and prograded across, and loaded, sandy and muddy

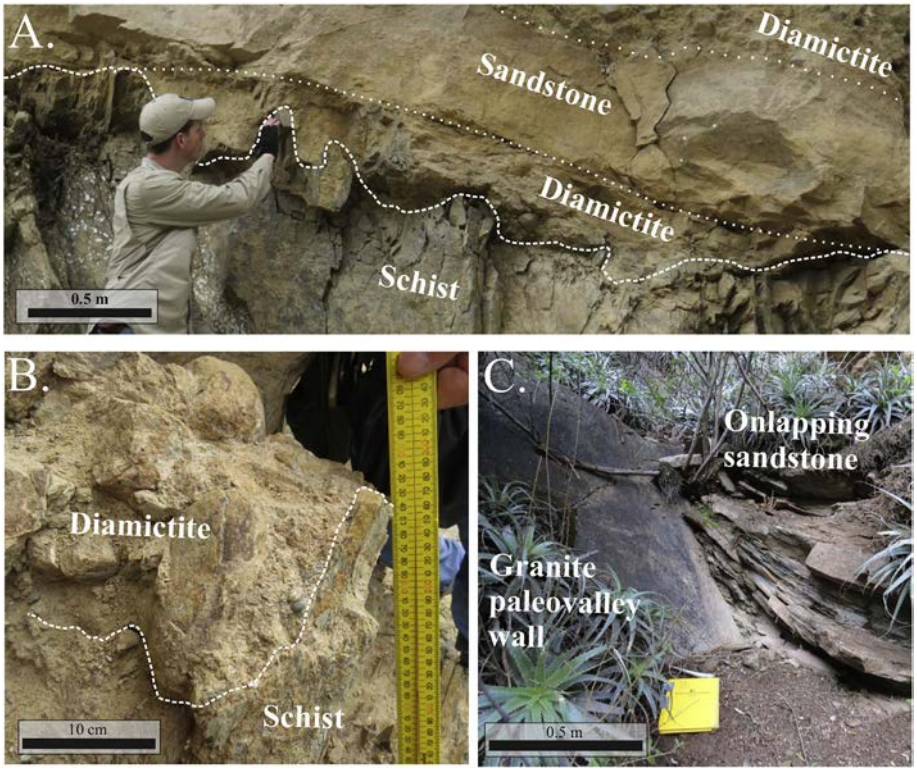

Fig. 6. (A) The nonconformity between clast-rich sandy diamictite and the schist basement at section OV1, which exhibits (B) thin slabs of schist protruding into the overlying diamictite, and (C) sandstones onlapping the steep (~65°), unstriated granite paleovalley wall at section OV8.

lacustrine deposits (cf. Colombo et al., 2009).

2.2. Facies B: sandy conglomerate

2.2.1. Facies B: sandy conglomerate description

Sandy conglomerates occurs in sections OV9 to OV12 where a thick succession (> 40 m thick) of conglomerate originates from a tributary paleovalley (Fig. 2B) and extends down the main paleovalley for over 400 m (Fig. 8A). The conglomerates occur as wedge-shaped downlapping beds that thin and fine westward where they grade into, and interfinger with, graded sandstone beds and laminated mudstones of Facies D, and sandstones containing symmetrical ripple marks, of Facies G (Fig. 8A and B), some of which have flat-topped crest. The lower termination of each successive downlapping clinoform steps up in elevation and extends farther toward the west along the outcrop as it interfingers with underlying sandstone (Fig. 8B). Upward, the sandstone and mudstone beds disappear and the succession becomes entirely a boulder conglomerate (Fig. 8A and B). Diamictites of Facies A also occur within these deposits and either grade or interfinger with the sandy conglomerates. Individual conglomerate beds rest on erosional, sharp and loaded bases. The conglomerate is reddish-tan in color, and beds range up to several m thick. The beds are generally internally massive, except where they display normal grading as they transition into overlying horizontally-laminated and graded sands of Facies D (Fig. 8C). The conglomerate is typically clast-supported with coarse sand filling the void spaces between the clasts (< 10% mud; Fig. 8A and D). Clasts are predominantly subrounded and granitic in composition, with common occurrences of quartzite and schist clasts. The conglomerates vary from boulder-rich with clasts up to 9.0 m in diameter (section OV9) to cobble-rich. Conglomerates also issue from at least one other tributary paleovalley that enters the main Olta paleovalley approximately 1.9 km to the east of section OV9 (Fig. 2B).

The sandy conglomerate facies also occurs between sections OV4 and OV5 where beds of conglomerate, 0.2–1.7 m thick, are interstratified with thick sandstone beds and laminated mudstones of Facies D and sandstones containing symmetrical ripple marks of Facies G. These conglomerates are deformed and will be described further with strata of Facies H.

2.2.2. Facies B: sandy conglomerate interpretation

This facies represents deposition from sheet flooding, noncohesive sediment gravity flows, and coarse-grained debris flows (cohesive sediment gravity flows) associated with alluvial fans and fan deltas (cf. Nemec and Steel, 1984, 1988; Blair, 1987, 2001; Blair and McPherson, 1994) that interfinger laterally with lacustrine deposits of Facies D and G. Deformation at the base of the conglomerates and debrites (Facies A) are the result of loading of material on water-saturated substrates in a subaqueous setting. Alluvial fans are common at the base of mountain valleys where steep-gradient, high-energy tributary streams rapidly deposit coarse-grained bedload during an abrupt reduction in stream gradient upon reaching the main valley floor. These fan- or cone-shaped deposits of alluvium are termed fan deltas where they terminate in a standing water body and deposition is mainly or entirely subaqueous (Nemec and Steel, 1988). Such lakes can occur in narrow valleys where fans and fan deltas prograde across the valley and impound drainage (Andreis et al., 1986; Colombo et al., 2009). Progradation is indicated by the increase in boulder conglomerate upward within the succession, and the westward stepping, downlapping, clinoforms. Deposition was dominated by event sedimentation during high-discharge flood events and debris flows. Normal grading in upper portions of beds reflects the waning stages of discharge and transport by low-density fluids. Clast may have also been supplied by rock fall from the valley walls.

In the Olta paleovalley, thick deposits of conglomerate emanate from tributary paleovalleys and extend outward into the main paleovalley (Figs. 2 and 8A). Conglomeratic clinoforms that downlap onto and interfinger with sandstones (Facies G) containing flat topped ripples suggest that the fans prograded out into and across a shallow water body. The upward stepping nature of the downlapping conglomeratic

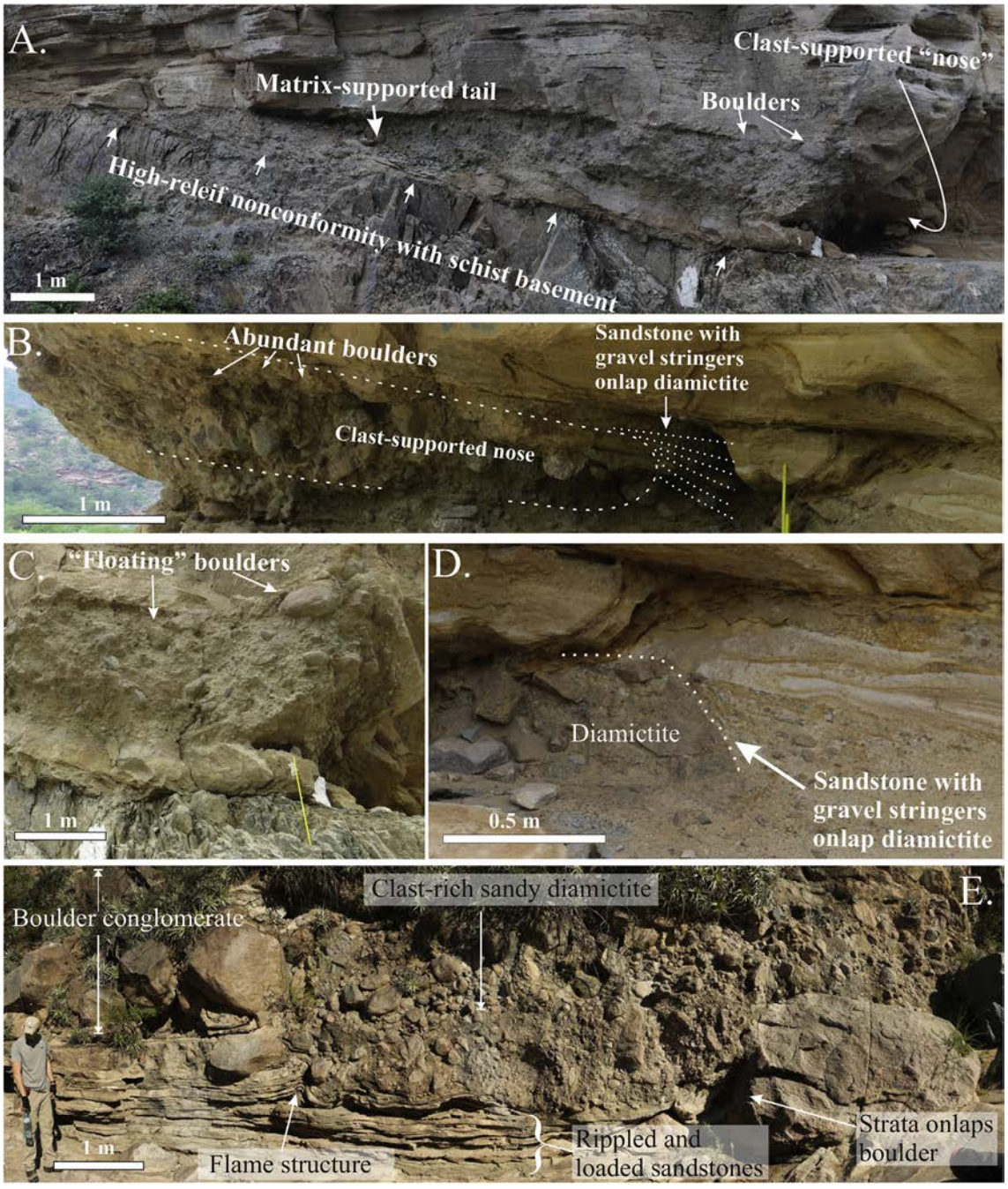

Fig. 7. A clast-rich sandy diamictite bed overlying schist basement at section OV1 with (A) a wedge-shaped profile and "floating" granite boulders protruding through the upper contact of the bed, (B) and (C) boulder-rich, clast-supported "nose" of the unit, and (D) coarse-grained sandstone with gravel stringers onlapping the steeply-dipping margin ("nose") of the diamictite. (E) Massive to inversely graded, clast-rich, sandy diamictite resting on and loaded into rippled sandstone (section OV10). The diamictite grades vertically into a cobble to boulder-rich conglomerate. Both the sandstone and diamcitite units onlap m-scale boulders.

clinoforms indicates that water levels in the paleovalley rose during fan deposition (Fig. 8A and B). The Olta paleovalley is less than 200 m wide in the area between sections OV7 and OV12 where a "paleo-tributary" enters the main valley (Fig. 2B). Therefore, progradation of these fans into and across the main paleovalley would have impounded drainage producing lakes as evidenced by lacustrine sediments that interfinger with distal alluvial fan conglomerates along the paleovalley, especially near sections OV8 and OV9 (cf. Colombo et al., 2009). In contrast, Socha et al. (2014) identified these conglomerates as diamictites with strongly-developed clast fabrics (Fig. 8) and interpreted these deposits as subglacial tillites. However, those authors noted the conspicuous absence of several diagnostic glacial features that were also not observed in this study including fine-grained matrix material, and clasts exhibiting polish, striations, or facets. However, clast fabrics also develop from streamflow and debris flows in alluvial fan deposits. No clear preferred orientations of clasts were observed for the conglomerates in this study. Conglomerates in the Olta paleovalley and its tributaries are bedded, and downlap and interfinger with sandstones in the main paleovalley, thus strengthening the interpretation that these units were deposited as alluvial fans and fan deltas.

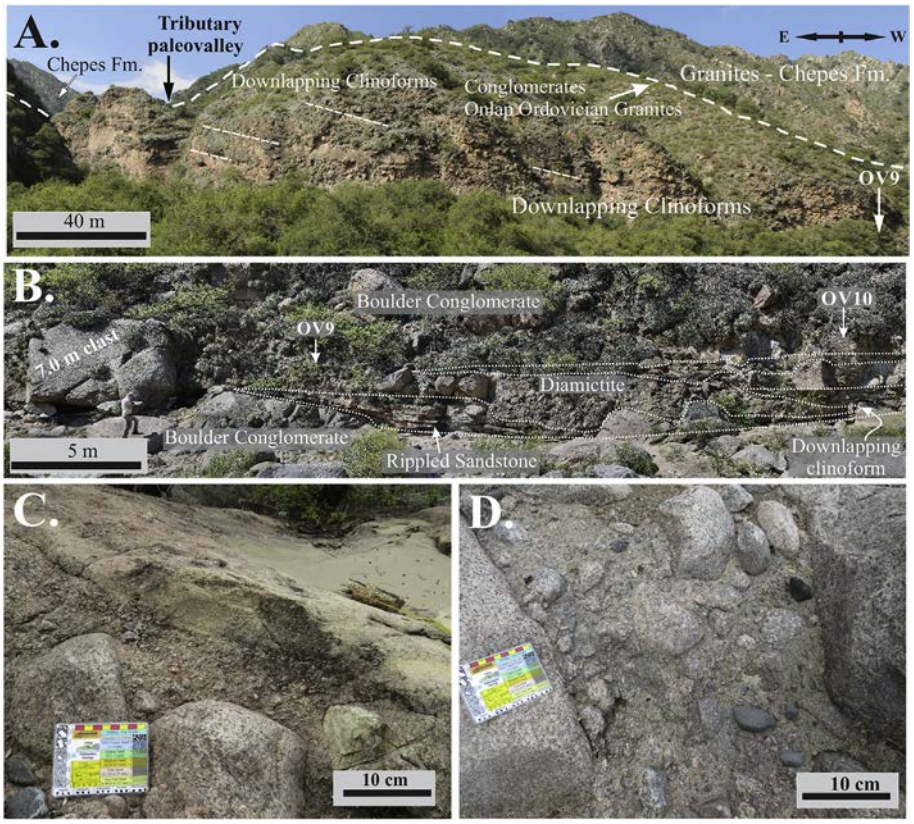

Fig. 8. (A) Sandy conglomerates of Facies B in the central portion of the Olta paleovalley where a +40-m outcrop of sandy conglomerates with downlapping clinoforms is exposed at the mouth of a tributary paleovalley near section OV9. (B) Wedge-shaped beds of conglomerate interfinger with and wedge out into horizontally-laminated sandstones of Facies D. Locations of columns OV9 and OV10 are marked. (C) Conglomerate with a normally graded top overlain by very coarse-grained sandstone and (D) conglomerate at the base of section OV9 consisting of subrounded granite clasts in a coarse sand matrix.

2.3. Facies C: boulder breccia

2.3.1. Facies C: boulder breccia description

Clast-supported breccias were observed at section OV7 less than 70 m from near-vertical granitic paleovalley walls on both sides of the paleovalley (Fig. 5B and C). At this site, angular granite boulders are chaotically stacked on top of each other (Fig. 9A). The upper, lower, and lateral contacts of this deposit were not exposed, but the matrix between boulders consists of very thin beds of heavily deformed, cohesive mudstone and fine-grained sandstones that include the deformed, but identifiable trace fossil *Diplopodichnus biformis* (Fig. 9B), suggesting that the unit overlies and laterally contacts Facies D. The +8.2-m thick unit lacks internal organization or stratification. Clasts are predominantly boulder-sized, including individual clasts up to 5 m in diameter, and typically the clasts display high angle (> 20°) to vertical orientations of their long axis.

2.3.2. Facies C: boulder breccia interpretation

The boulder breccia observed at section OV7 is interpreted as direct rock fall off valley walls into soft lake sediment. Exposures of the Olta paleovalley walls possess slopes that commonly exceed 60° and approach vertical in many places (Fig. 5). An exposed granite surface directly contacting lacustrine deposits less than 70 m away from the breccia outcrop suggests that this deposit rests against a steep portion of the wall. Clasts are largely angular and match the composition of the local bedrock, suggesting short transport distances. The arthropod grazing trace *Diplopodichnus biformis* has been reported in deposits from multiple late Carboniferous water bodies, including fjord environments in the western Paganzo basin (Schatz et al., 2011), glacial lakes in the Paraná basin of Brazil (Netto et al., 2009), and in the Teresina Fm. in southern Brazil where a benthic marine fauna was likely stressed by salinity fluctuations (Lima and Netto, 2012). The occurrence of trace-fossil bearing sandstones squeezed between the boulders suggests that the rock avalanche occurred into an existing water body, and that the lake sediment was deformed/squeezed up into the voids between the clasts during the rock fall. Rockfall events are also catalysts for lake development in narrow mountain valleys (cf. Colombo et al., 2009).

Fig. 9. (A) A boulder breccia unit exposed at section OV7 that contains highly deformed sandstone and mudstone squeezed between angular granite boulders. (B) The deformed sandstone contains *Diplopodichnus biformis* traces exposed on a near vertical bedding plane contained between breccia clasts.

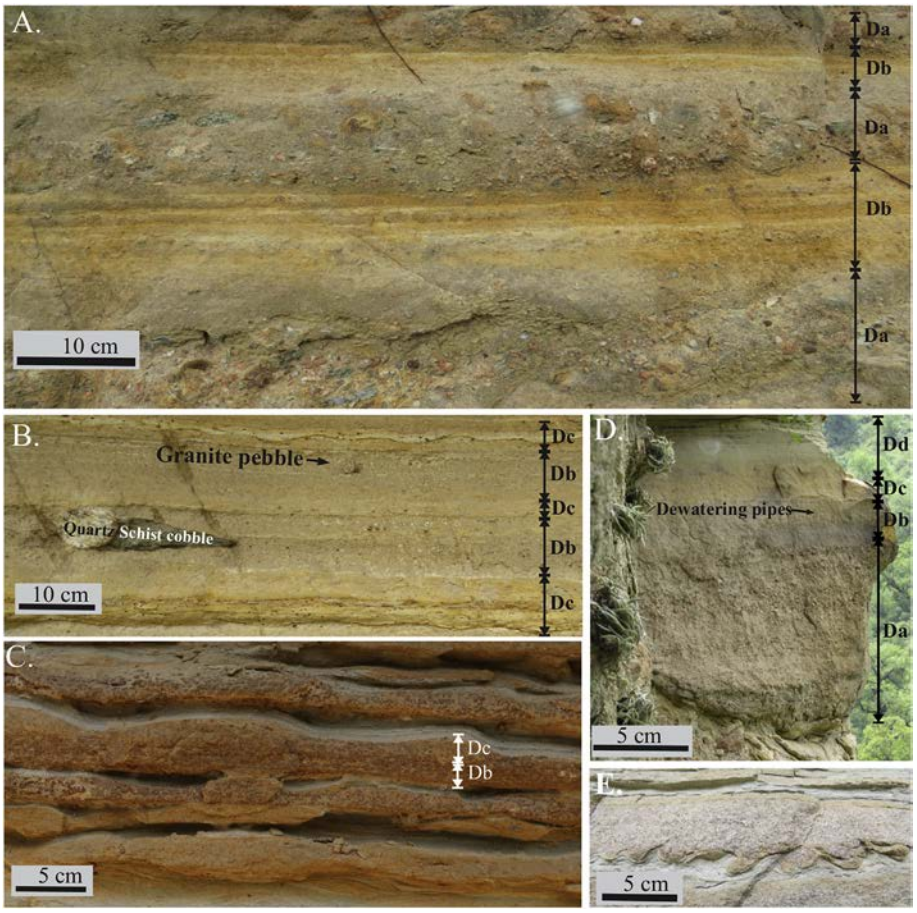

Fig. 10. (A) Alternating beds of graded gravelly coarse-grained sandstone (Subfacies Da) and horizontally-laminated medium-to coarse-grained sandstone (subfacies Db) at the base of section OV2. (B) Upper portions of OV2 are dominated by subfacies Db interbedded with minor current ripple cross-laminated fine-grained sandstone (subfacies Dc), which becomes the dominant subfacies represented in section OV3. (C) Graded sandstones from section OV4 showing horizontally laminated medium sandstones (subfacies Db) grading upward into cross-laminated medium to fined-grained sandstone displaying round crested combined flow ripples. Very-fine-grained sandstone and siltstone drape the ripples. (D) A fining-upwards sequence showing all four subfacies overlying (section OV4). (E) Load and flame structures (E) commonly occur where subfacies Db overlies subfacies Dd.

2.4. Facies D: graded sandstone

2.4.1. Facies D: graded sandstone description

The graded sandstone facies consists of sandstone packages that contain one or all of the following subunits: (Da) thin to medium beds of massive or graded, gravelly coarse-grained sandstone, (Db) thin beds of horizontally-laminated, coarse-to medium-grained sandstone, (Dc) thin beds of current ripple cross-laminated, medium-to fine-grained sandstone, and/or (Dd) medium laminations to thin beds of parallel-laminated, siltstone to very fine-grained sandstone (Fig. 10). Lower portions of sections OV1-OV3 (Fig. 2) show repeating 15–40 cm thick Da/b sandstone packages with abundant pebbles, cobbles, and occasional boulders (Fig. 10A). These lower units overlie bedrock or clast-rich sandy diamictites of Facies A with sharp or erosive contacts and the sandstones also onlap the nose of a wedge-shaped diamictite bed at section OV1 (Facies A; Fig. 7B and D). Individual Da/b packages (Fig. 10A) are laterally continuous across the exposures; slightly thinning and fining in the direction of paleoflow (~220°). These beds transition upwards to 10–25 cm thick Db/c couplets that generally fine and thin upwards to 5–15 cm Db/c/d packages (Fig. 10A, B, and 10C).

Sections OV4 and OV5 are dominated by 10–30 cm Db/c/d packages (see Facies H) except where 10–50 cm Da/b or Da/b/c/d beds (Fig. 10D) gradationally overlie massive sandy conglomerate beds (Facies B). Beds are laterally continuous over distances across the exposures (up to 50 m). Upper portions of section OV4 show very thin beds of rippled fine- (Dc) and very fine-grained sandstone (Dd) grading upward into horizontally-laminated mudstone of Facies E. Upper portions of Sections OV1, OV4, and OV5 commonly show asymmetrical, symmetrical, and combined flow ripples (Fig. 10C; see Facies G). The base of medium-grained horizontally-laminated sandstones (Db) commonly contain prod and bounce (sole) marks where they overlie siltstone (Dd). These sandstones and siltstones occasionally show small-scale (< 5 cm) load and flame structures (Fig. 10E) and dewatering pipes penetrating horizontal laminations (Fig. 10D), and *Diplopodichnus biformis* trace fossils are common on the top surface of rippled sandstones. Outsized pebbles and cobbles are common in coarse-grained sandstones of this facies and are occasionally present in finer-grained units.

2.4.2. Facies D: graded sandstone interpretation

Together these deposits have sedimentary structures similar to deposits of high- and low-density turbidity currents (divisions A/B/C/D of Bouma, 1962; $T_A/T_B/T_C/T_D$ of Talling et al., 2012; representing Da/Db/Dc/Dd), and flood related units deposited in shallow water basins by hyperpycnal flow (cf. Mulder and Chapron, 2011; Zavala et al., 2006, 2011). Turbidity currents can be triggered from cohesive debris flows (Sohn, 2000; Talling et al., 2012), which is the interpretation for thick units that directly overlie or onlap debrites in sections OV1, OV4 and OV5 (Fig. 7B and D). Lacustrine "turbidites" are more commonly referred to as hyperpycnites that owe their origin to high river discharge during flood events (Dadson et al., 2005; Talling, 2014), prograding delta-fronts, or due to delta-lip failures (Lambert and Giovanoli, 1988; Zavala et al., 2006, 2011; Girardclos et al., 2007). The predominate absence of mud and common wave-influence structures observed in this facies in the eastern sections of the paleovalley suggests deposition in relatively shallow portions of a lake above storm wave base. The turbidites/hyperpycnites could also be triggered by storm activity and could be considered potential storm deposits. A deepening of the lake through time likely occurred as coarse-grained units dominate basal sections of the paleovalley and show a gradual fining and thinning of units upwards until the succession is dominated by mudstone of Facies F.

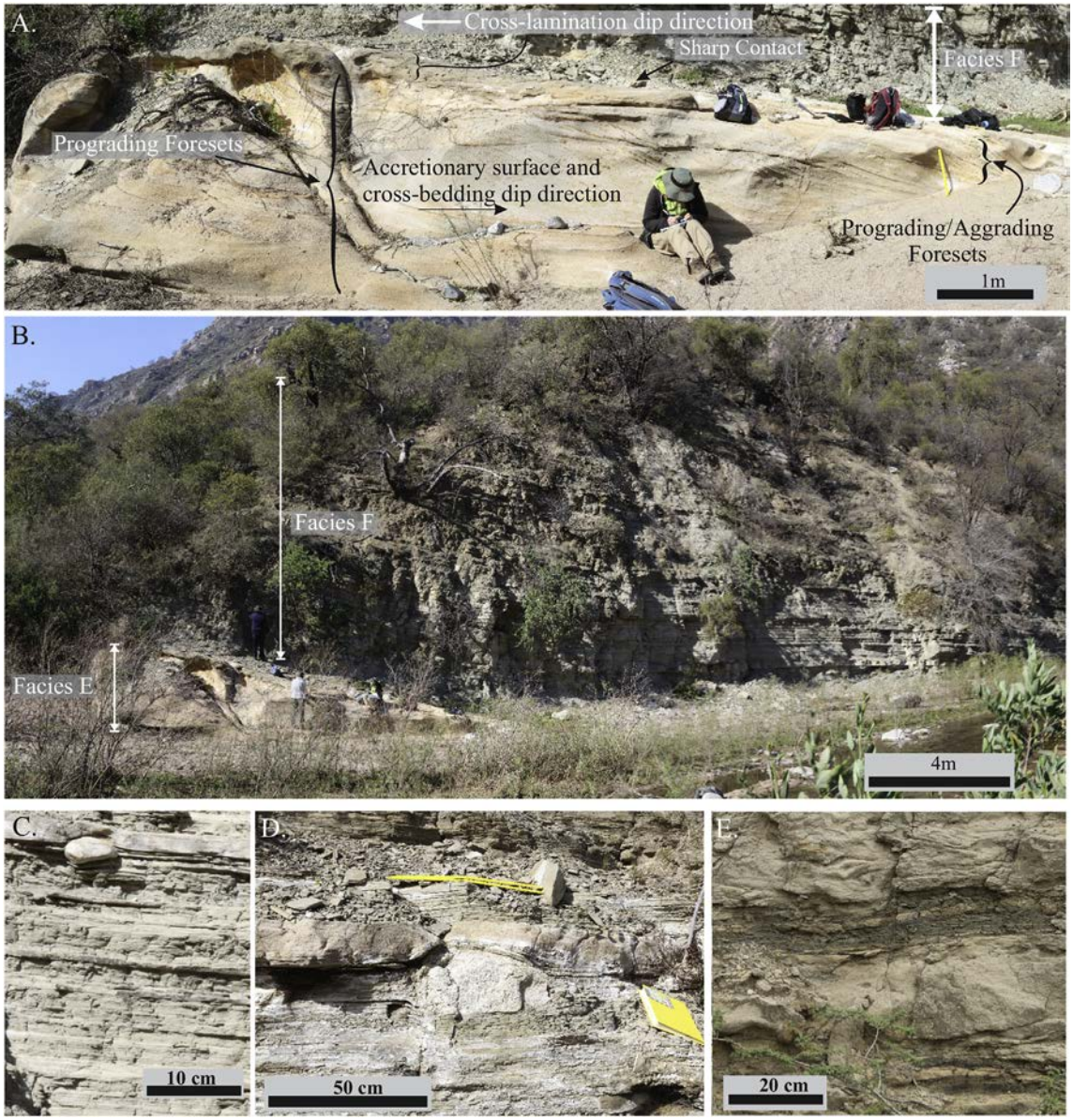

Fig. 11. (A and B) Medium-to Coarse-grained sandstone containing sigmoidally-shaped foreset beds of Facies E overlain by interbedded graded sandstones (Facies D) and laminated mudstones of Facies F at section OV14. A sharp surface separates sandstone in Facies E from Facies F. Laminated mudstone increase in abundance upward within Facies F. (C) Alternation of mudstone and sandstone near the base of facies F at section OV14. Note the occurrence of a rare outsized clast. (D) Interbedded mudstone and sandstone with a bed of hummocky-like cross bedding and a rare outsized clast of weathered granite (section OV14). (E) Interbedded laminated mudstones and sandy clinoforms (Facies I) at the base of section OV16.

Similar turbidity current/hyperpycnite-dominated lacustrine deposits occur in the nearby Malanzán paleovalley (Andreis et al., 1986; Buatois and Mángano, 1995) and the western Paganzo basin (Limarino et al., 1984; Buatois and Mángano, 1994). The outsized clasts commonly observed in these deposits can be transported by the flow itself (Postma et al., 1988) or by a variety of mechanisms including ice rafting (iceberg, lake ice, or anchor ice), rafting by vegetation, and as outrunner clast or clasts left behind during sediment bypass of waning sediment gravity flows (see Facies E interpretation; cf. Andreis and Bossi, 1981; Thomas and Connell, 1985; Woodborne et al., 1989; Gilbert, 1990; Dionne, 1993; Bennett et al., 1994; Kempema et al., 2001; Carto and Eyles, 2012). Bouncing clasts could also be projected into the lake during rock fall events off the steep valley walls.

2.5. Facies E: medium to coarse-grained cross-bedded sandstone

2.5.1. Facies E: medium to coarse-grained cross-bedded sandstone description

Medium-to coarse-grained, trough, cross-bedded sandstone (> 2 m thick) occurs at the base of section OV14 (Figs. 2B and 4C), and consists of a series of westward-dipping cross sets (0.1–0.5 m thick; Fig. 11A). The largest sets occur at the base of the sandstone and decrease in thicknesses upward. The sets display an aggradational/progradational, sigmoidal-shaped geometry (cf. Galloway, 1989) with downstream accreting surfaces dipping up to 15° towards the west. The top of the exposed sandstone body consists of a 0.3 m thick erosionally based, fine-to medium-grained, trough, cross-laminated sandstone that contains multiple sets that dip to the east (Fig. 11A). A sharp surface separates cross-stratified sandstone below from cm to dm thick interbeds of mudstone and very fine-to medium-grained, graded sandstone beds

above (Facies D and F; Fig. 11A and B). Sandstones in Facies F are horizontally and trough cross-laminated, and grade upward into laminated mudstone with rare dropstones (Facies F; Fig. 11B, C, 11D, and 11E).

2.5.2. Facies E: medium to coarse-grained cross-bedded sandstone interpretation

Facies E is exposed at section OV14 located 800 m to the west (in the direction of paleoflow) of exposures of the Sandy Conglomerate Facies (Facies B), which are interpreted as an alluvial fan/fan delta succession that prograded out of, and away from, a tributary paleovalley located between sections OV8 and OV9 (Fig. 2). The proximity of the two facies suggests a lateral relationship between the two. Sandstone in Facies E is similar to sands deposited as bedload, flood-dominated, fluvial braid bars, fan-delta lobes, or delta mouth bars (cf., Mutti et al., 1996; Best et al., 2003; Bridge and Lunt, 2006; Mulder and Chapron, 2011; Zavala et al., 2011). These similarities include: 1) sigmoidal-shaped cross-bed foresets, upward decreases in the thickness of cross-bed sets, and an upward fining grain-size trend, all of which suggest deposition from a waning high-velocity flow (Mutti et al., 1996); 2) a lack of internal fine-grained drapes or wave rework structures, which suggest an absence of episodic flow fluctuations during deposition of the sediment body; and 3) the occurrence of both prograding and aggrading cross-bed set geometries, which could result from either a rise in base level, or deposition do to the waning nature of the flow (cf. Galloway, 1989; Mutti et al., 1996). Regardless of which of the above interpretations is correct, all three environments represent either subaerial or shallow-water deposition that could easily be a downstream equivalent to the prograding fan/fan delta exposed in sections OV9 to OV12. The upward fining mudrock succession (Facies F) that overlies Facies B indicates ultimate submergence of the bar/lobe and progressive deepening of waters within that portion of the paleovalley. Eastward dipping fine-to medium-grained, cross-laminated sandstone resting erosionally on the bar/lobe top could have formed do to wave reworking during rising water levels, or could have formed due to reflection of the original flow off the valley walls (cf. Hiscott and Pickering, 1984).

2.6. Facies F: laminated mudstone

2.6.1. Facies F: laminated mudstone description

This facies consists of thin, horizontal laminations of mud and silt, which occur in beds up to 0.2 m thick in the uppermost portion of section OV4 where it is interbedded with fine-grained, graded sandstones of Facies D. In the western portion of the Olta paleovalley the facies occurs in a +8.0 m thick succession (section OV14 and OV15; Fig. 2) above a flooding surface on top of sandstones of Facies E (Fig. 11). There, laminated mudstone interbedded with thin graded sandstone beds and occasional beds of hummocky cross-stratification at the base of the succession grade upward into thick mudstone with occasional beds of horizontally-laminated, very fine-grained sandstone up to 2 cm thick (Fig. 11). In section OV16 and OV18 beds up to 0.2 m thick intercalate with sandy clinoforms in a coarsening-upward succession at the base of Facies I (Fig. 11E). Laminae are even and continuous, ranging from 1 to 5 mm in thickness and are rarely disrupted by rare granule-to boulder-sized outsized clasts (Fig. 11C and D). Impressions of fossil plants, including *Cordaites* sp., also occur on silty bedding planes.

2.6.2. Facies F: laminated mudstone interpretation

The fine-grained sediments of this facies record deposition below normal wave base in either a lacustrine (east end of the paleovalley) or marine (west end of the paleovalley) environment. The thin sandstone deposits at the base of the mudstone succession in section OV14 were likely deposited as hyperpycnal flow or reworked sands due to storm activity. The flooding surface and fining upward succession at this site suggest deepening of waters in the paleovalley. Gutiérrez and Limarino (2001) identified acritarchs from these mudrocks that they interpreted to be affiliated with brackish marine conditions, which suggest that these deposits were associated with a Late Mississippian-Early Pennsylvanian transgressive event in western Argentina. Very thin beds of very fine-grained sandstone observed in section OV15 are less than 400 m laterally from exposures of Gilbert delta bottomsets observed in section OV16 and likely represent deposition from distal hyperpycnal underflows (Lambert and Giovanoli, 1988; Crookshanks and Gilbert, 2008). Similar intervals of mudstone have been described in the Malanzán paleovalley (Andreis et al., 1986; Buatois and Mángano, 1995) where pebbles and cobbles are interpreted as dropstones and cited as the primary evidence for glacial influence in the valley; however, as discussed previously, multiple non-glacial processes can transport outsized clasts in lake or marine waters in such narrow valleys. Sterren and Martínez (1996) suggested the diminutive flora that existed in the paleovalley were incapable of rafting large clasts, and reported the existence of clasts with extrabasinal lithologies, which suggest glacial transport. However, Sterren and Martínez (1996) did not mention the lithologies of these exotic clasts, and clasts representative of sources other than local basement rocks were not observed in this study. Andreis and Bossi (1981) and Andreis et al. (1985) considered outsized clasts as evidence for seasonally frozen lake surfaces which could accumulate sediment from tributaries and mass wasting off the valley walls during the winter months and subsequently raft clasts upon ice break-up. Sections containing these mudrocks are located adjacent to the high relief nonconformity defining the valley walls, suggesting direct rock fall into the lake was also possible. The absence of glacial features on the clasts themselves (i.e., bullet shape, striations, and/or facets), including the absence of extrabasinal clast lithologies anywhere within the studied section, is consistent with non-glacial transport mechanisms for the outsized clasts.

2.7. Facies G: symmetrically rippled and bedded sandstone

2.7.1. Facies G: symmetrically rippled and bedded sandstone description

Successions of asymmetrically-rippled sandstones (Facies D) are interrupted by intervals of variable thicknesses of sandstone (0.1 to +5 m) that show symmetrical to quasi-symmetrical ripples of Facies G, which comprises the majority of upper portions of several sections (OV1, OV4-OV6, and OV8; Fig. 2). In these sections, Facies G gradationally overlies horizontally-laminated coarse-to medium-grained, graded sandstones of Facies D and is interbedded with sandy conglomerates of Facies B. In more vertically extensive stratigraphic exposures (such as OV4), sandy units thin upward while silt drapes on top of rippled beds thicken, resulting in a gradual transition to mudstones in Facies F. Individual beds show sharp upper and lower contacts and are laterally continuous across exposures. This facies is superficially similar to fine-grained packages of Facies D in that these intervals are characterized by thin to thick beds of medium-grained sandstones that are horizontally laminated and abruptly grade upward into fine-grained sandstones that are ripple cross-laminated. Rippled beds are commonly overlain with very thin beds of parallel-laminated, very fine-grained sandstone and siltstone (Fig. 12A), but can be distinguished from Facies D by the occurrence of symmetrical and weakly-asymmetrical ripples that are present at the top of medium-grained sandstone and throughout fine-grained sandstone beds. Internally, the symmetrical ripples display either superimposed vertically climbing symmetrical ripples within m thick successions (section OV6; Fig. 12B), or unidirectional cross-laminations that are anomalous to the profile of the overlying bedform (e.g., section OV4). Occasional pebble-sized outsized clasts are present and *Diplopodichnus biformis* traces occur.

2.7.2. Facies G: symmetrically rippled and bedded sandstone interpretation

Symmetrically-rippled sandstones represent wave-modification of sands deposited by turbidity or hyperpycnal currents in shallow areas of

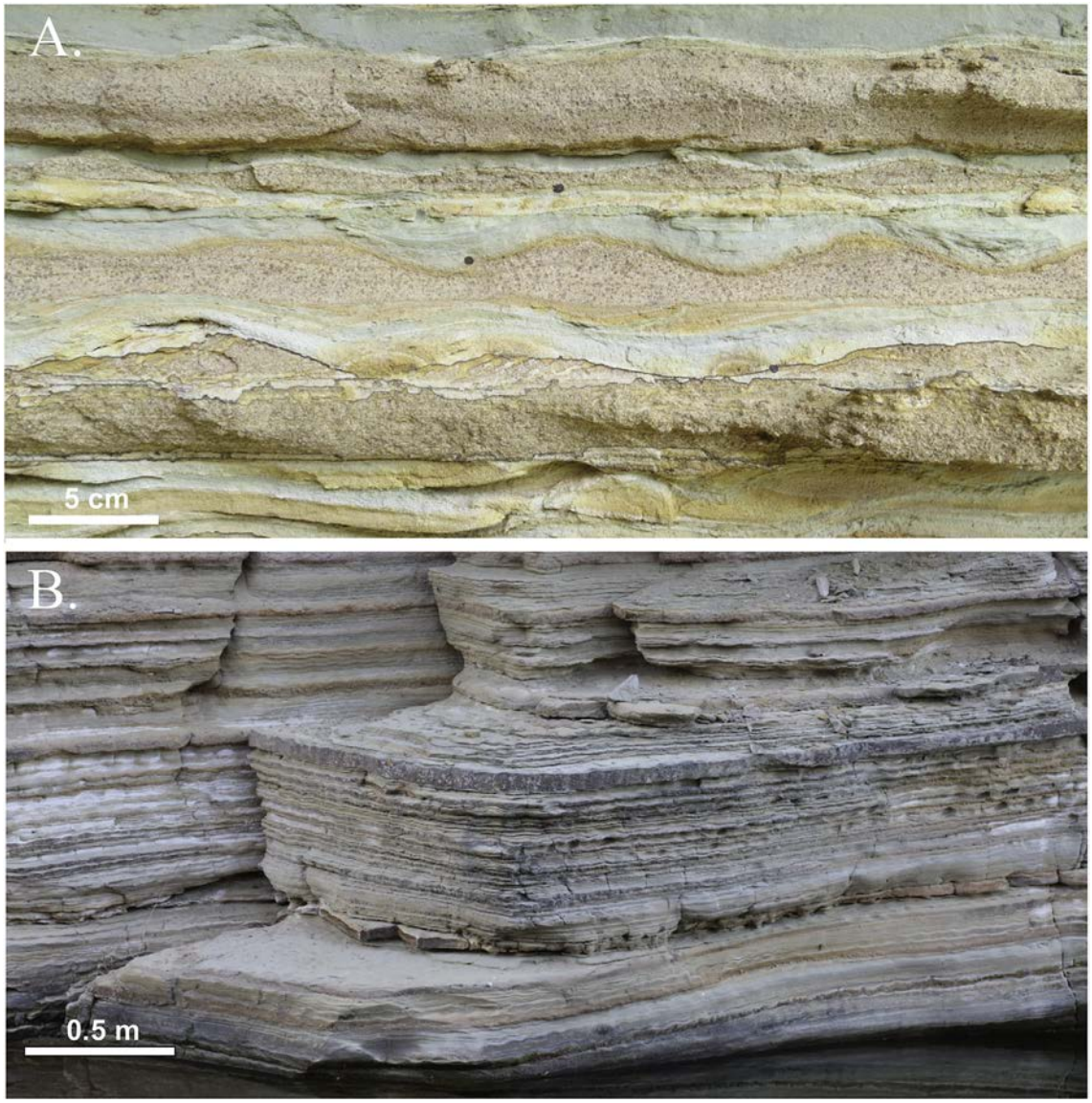

Fig. 12. Symmetrical and weakly-asymmetrical rippled sandstones of Facies G observed in (A) section OC5, where cross-laminations in the reddish-brown medium-grained sandstone are unidirectional. (B) Section OV6 exposes a thick succession of climbing symmetrical ripples alternating with horizontally laminated sandstone. (For interpretation of the references to color in this figure legend, the reader is referred to the Web version of this article.)

the lake. The internal structure of the ripples suggests either reworking of an original unidirectional flow deposit, or complete reworking by bi-directional wave activity (climbing wave ripple successions). Buatois and Mángano (1995) suggested similar deposits from the Malanzán paleovalley represent reworking of turbidites/hyperpycnites by storm waves, but the continuity of individual beds and lack of hummocky cross-stratification suggest minimal influence from high-energy storm events. Ripple Indices are highly variable in this facies and suggest sedimentation under combined flow regimes where both unidirectional currents and wave activity are superimposed on the deposits. Hummocky cross-stratification can form in lakes, and occurs in Facies F. However, the narrowness of the valley and potentially shallow water depths would have likely inhibited the formation of large amplitude waves within this depositional environment (cf. Syvitski et al., 1987; Boulton, 1990).

2.8. Facies H: folded sandstone and mudstone

2.8.1. Facies H: folded sandstone and mudstone description

This facies includes three distinct types of deformation, which consist of 1) conglomerate load and associated sandstone and mudstone flame structures, 2) loaded sandstone and mudstone beds beneath conglomerates and diamictites (see Facies B), and 3) localized decimeter to meter-scale folds that resemble dropstone ruck structures (cf. Thomas and Connell, 1985), which are associated with boulder-sized clasts.

Laterally continuous horizons of deformed sandstones, mudstones (Facies D, F, and G), and granule-to boulder-conglomerates (Facies B) up to 1.8 m thick occur in sections OV4 and OV5 (Figs. 2B and 13). These horizons are bounded above and below by undeformed beds. The deformation consists of sandstone and mudstone flame structures alternating laterally with conglomerate loads and pseudonodules every 1–4 m along the length of the exposures. The base of the zone is only mildly deformed with gentle open folds, but deformation increases upward where finer-grained beds show tight folds and are, in places, brecciated (Fig. 13A, B, 13C, 13D, and 13E). These strata are extruded upward into the overlying conglomerate and form large flame structures that, in some places, penetrate the overlying conglomerate (Fig. 13D and E). Orientations of the flame structures are highly variable, and in a few places, the loads are detached from the conglomerate

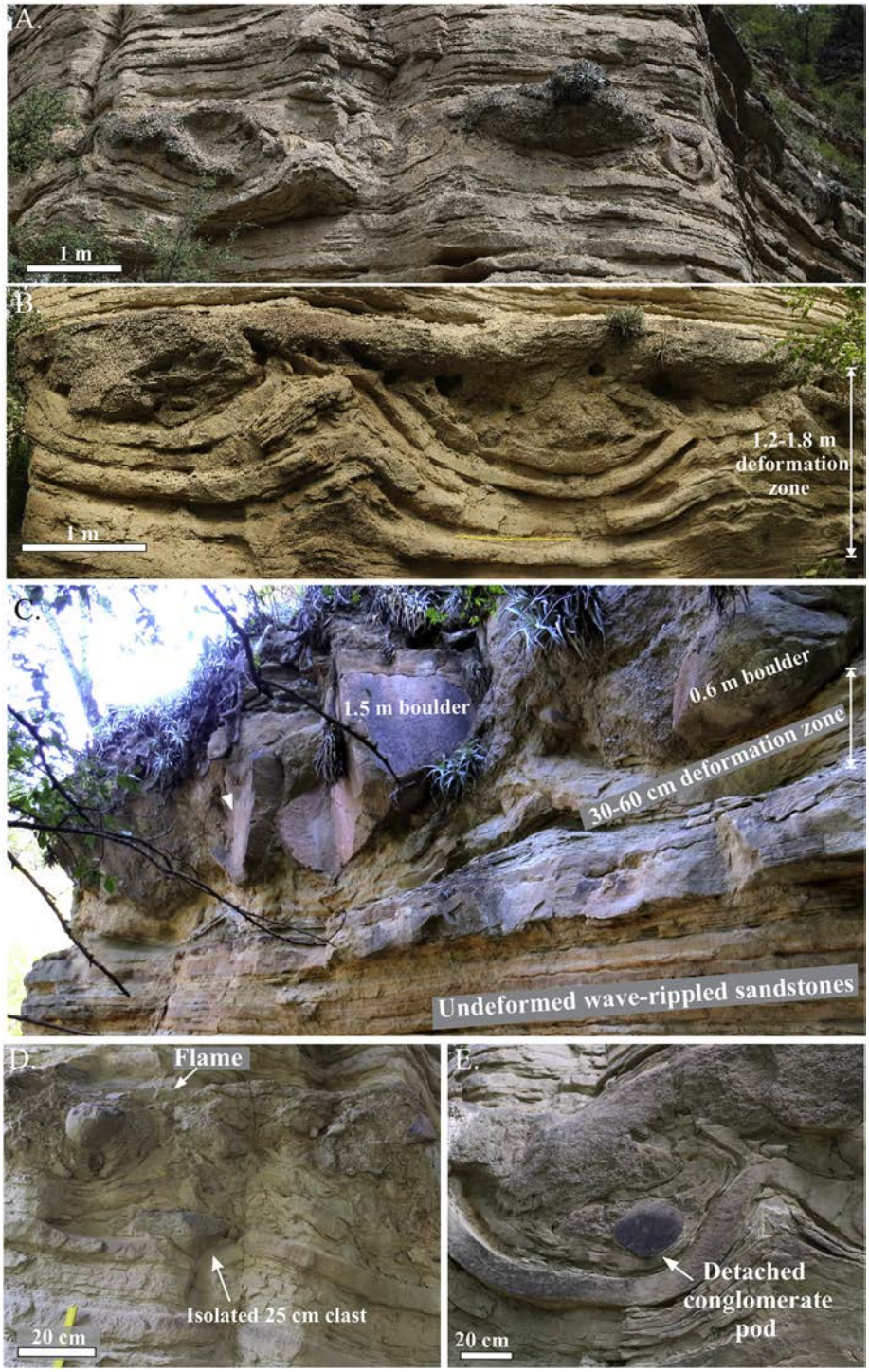

Fig. 13. Deformed sandstones and mudstones that occur in laterally continuous horizons (A; Section OV4) below conglomeratic load structures at (B) the base and (C) upper portions of section OV5. (D) Isolated clasts and (E) conglomerate pods are occasionally detached from the overlying conglomerate (Section OV5).

and form isolated pods (pseudonodules) of conglomerate in the underlying sandstone (Fig. 13E). These deformed horizons can be traced for several hundred meters within the main paleovalley, and similar load and flame structures contained entirely within a thick succession of symmetrically rippled sandstone (Facies G) occur 600 m to the west in section OV6. At least three different deformed horizons occur in the area that extends from section OV4 to section OV6.

Between sections OV9 to OV11 (Fig. 2B), deformed, interbedded sandstones and mudstones interfinger with, clast-rich, sandy, matrix- and clast-supported boulder conglomerates and diamictites of Facies A and B. The coarse clastic beds thin laterally towards the west (sections OV11 and OV12), and the deformed intervals of sandstone and mudstone also disappears in the same direction transitioning into m-thick, undeformed sandstone and mudstone successions (Facies D and Facies F). Locally, the interbedded sandstones and mudstones are deformed beneath diamictites and conglomerates lenses, and around m-scale boulders (Figs. 7E and 14). Individual boulders penetrate the sandstone and mudstone beds. The deformation consist of internally folded, diapiric-like structures up to 0.8 m in height and 1 m in width that protrude upward around the margins of boulders, between boulders, and

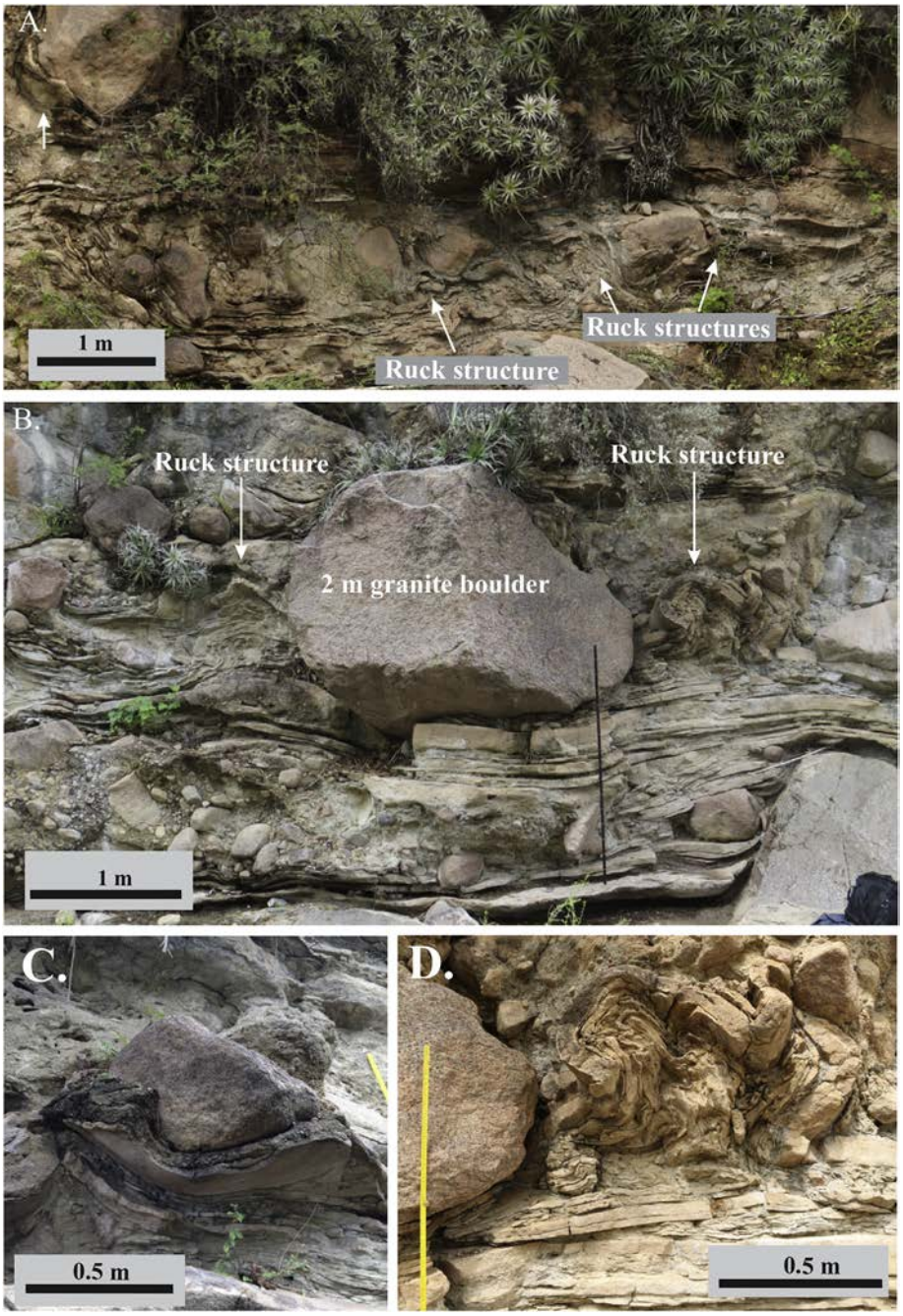

Fig. 14. (A) Discontinuous deformed zones containing multiple "ruck structures" (arrows) and "depression bowls" surrounding boulders. Note the relatively undeformed sandstone above and below the deformation zone, and that multiple isolated deformation zones occur within the interbedded sandstones and mudrocks (strata are located between sections OV10 and OV11). (B) A granite boulder with associated sandstone and mudstone ruck structures at section OV9. (C) A granite boulder contained within a sandstone "bowl." (D) Detailed view of the ruck structure to the right of the granite boulder in Fig. 14B.

along the margins of the conglomerate and diamictite lenses (Figs. 7E and 14). Three-dimensional exposures reveal that some boulders are sitting in bowl-like depressions surrounded by circular diapiric structures (Fig. 14A and C). *Diplopodichnus biformis* and *Gordia marina* trace fossils occur on the upper surface of the sandstone beds.

2.8.2. Facies H: folded sandstone and mudstone interpretation

Gravel deposits at sections OV4 and OV5 were previously interpreted by Socha et al. (2014) as the result of subglacial sedimentation or proglacial debris flow deposition with deformation resulting from ice overriding these deposits and imparting a shear fabric with fold axes transverse to the trend of the valley, suggesting a westward ice flow direction. However, we found no faceted, striated, or polished clasts, horizontal/subhorizontal shear fabric, or down valley fold vergence in these or any other deposits in the paleovalley. Deformation was vertical in nature and was due to loading and liquefaction. Deformation of conglomerate, sandstone and mudstone at sections OV4 and OV5 is indicative of loading of dense conglomeratic material on water-saturated substrates. These strata were deformed due to liquefaction and failure of the substrate producing an extensive three-dimensional network of gravel loads and pseudonodules separated by diapiric/flame-like water escape structures that formed during or shortly following deposition. Multiple horizons that cross facies (Facies D and G) boundaries indicate that multiple liquefaction events influenced

multiple environments within the paleovalley. Seismic activity, landslides, loading, storm waves, and cyclonic and internal waves can produce load, pseudonodule and flame structures, all of which occur within the Olta paleovalley (cf. Alfaro et al., 2010; Shanmugam, 2016).

Socha et al. (2014) suggested that the thick succession of coarse clastics between OV9 and OV12 are the remnants of a recessional moraine. They interpreted the folded fine-grained sediments between clasts and conglomerates/diamictites (see Facies B) at the base of the section to be the result of subglacial deformation and/or dewatering of over-pressurized sediment being overridden by an advancing glacier. They also noted fold axes perpendicular to the assumed ice-flow direction. In marked contrast to the above interpretation, we interpret the folded sandstones and mudstones between sections OV9-OV12 as lacustrine sediments and observed that laterally, these deposits intercalate with conglomerates and diamictites (see Facies B) deposited by a prograding alluvial fan/fan delta (cf. Harvey, 1990; Blair and McPherson, 1994). In a wider context, an examination of specific folds identified as glacial deformation by Socha et al. (2014) suggests that they are load, flame, and ruck structures (cf. Thomas and Connell, 1985). These structures represent rapid loading of water-saturated lacustrine sediments by stream and debris flow events across distal portion of the alluvial fan/fan delta and by mass movement off the valley walls. The “ruck” structures, which occur on all sides of large boulders in section OV10 were also likely caused by rock fall off the narrow valley walls. Although Socha et al. (2014) reported folds with an apparent axis perpendicular to that of the valley, the ruck/diapiric structures are three-dimensional features with no down-valley vergence.

2.9. Facies I: sandy to gravely clinoform

2.9.1. Facies I: sandy to gravely clinoform description

The sandy to gravely clinoform facies occurs in the highest stratigraphic position in the westernmost portion of the study area (Fig. 4D). At sections OV16 and OV18 (Figs. 2 and 15), the outcrops display gently dipping (~0–10°), laterally extensive bottomset beds (Fig. 15B) that coarsen, thicken, and steepen laterally and vertically into foreset beds that dip between 10 and 35° in a down-valley direction towards the west and southwest. Basal portions of section OV16 contain 2–10 cm thick beds of very fine-grained sandstone and are variably intercalated with 1–20 cm beds of horizontally-laminated mudstone of Facies F. These beds are overlain by foreset beds comprised of very coarse-grained pebbly sandstone to granule conglomerates ranging from 0.2 to 2.3 m in thickness, which are typically massive or parallel-bedded with normal grading in the upper portions of beds. Near section OV16, the paleovalley is joined by a tributary paleovalley, and the main valley width changes dramatically from < 500 m to as much 1200 m in width (Fig. 2B). Deposits displaying clinoform geometries occur at the mouth of the tributary paleovalley and throughout the main portion of the Olta paleovalley. Across the width of both valleys, this facies occurs as offset stacked bodies displaying dipping clinoforms.

2.9.2. Facies I: sandy to gravely clinoform interpretation

The sandy clinoforms of this facies represent deposits of prograding Gilbert-type deltas and sedimentation by high-gradient streams depositing coarse-grained sediment into proximal lake or marine environments within the narrow paleovalley (cf. Stanley and Surdam, 1978; Colella et al., 1987). The occurrence of multiple offset but stacked clinoform-bearing bodies suggest compensational stacking of deltaic deposits that could keep pace with increases in accommodation during lake-level rise. Such stratal packages commonly occur at nodal points within a valley where valley widths change dramatically. At such sites, fluvio-deltaic deposition is capable of keeping pace with rapid increases in accommodation space (cf. Catuneanu, 2006).

3. Discussion

The difficulty in interpreting LPIA strata is largely a product of limited exposures, the difficulty of applying geomorphic principles to ancient deposits, and the difficulties in determining the origin of diamictites and strata deformed by soft sediment deformation. Late Paleozoic glaciation of the Precordilleran area and the Sierras Pampeanas in the Paganzo Basin is indicated by radial and westward directed ice flow indicators along the western portion of the basin, and by clast and sandstone composition in the same region that suggest derivation from these uplifted blocks (cf. López-Gamundí and Martínez, 2000; Kneller et al., 2004; Marenssi et al., 2005; Henry et al., 2008; Limarino et al., 2014). However, the extent of glaciation across the

Fig. 15. (A) A 38 m thick outcrop of sandy clinoforms (Facies G) exposed in section OV16 in the western portion of the Olta paleovalley. (B) Strata at section OV18 that contains extensive interstratified sandstone and mudrock bottom set beds and steeply dipping forest beds.

whole of the Paganzo Basin is unknown, especially in the eastern portion of the basin. The concept of widespread glaciation is based, in part, on the occurrence of a widespread, modern peneplain-like feature that occurs on elevated blocks throughout the Paganzo Basin (Astini et al., 2009; Astini, 2010). This surface is used to suggest that an extensive glaciated plateau extended across the whole basin during the Mississippian (325–340 Ma), and that this was followed by Early Pennsylvanian (~305–325 Ma) contraction of ice onto isolated uplifts during a change to back-arc spreading in a broken foreland basin (Astini et al., 2009; Astini, 2010). However, thermochronometric, stratigraphic, and geomorphic data suggest that the peneplain-like surface is a product of Mesozoic and Cenezoic erosion (cf. Jordan et al., 1989; Carignano et al., 1999; Enkelmann et al., 2014; Rabassa et al., 2014). The occurrence of a warm-temperate Serpukhovian (~326–331) paleoflora in the western part of the Paganzo Basin also suggests that glaciation was not continuous from 340 to 305 Ma (Balseiro et al., 2009; Gulbranson et al., 2010; Césari et al., 2011; Limarino et al., 2014).

A primary line of evidence for the interpretation of the Olta-Malanzán paleovalley as an ancient glacially carved valley/fjord is its present "U"-shaped profile (Socha et al., 2014). However, the modern Olta-Malanzán valley is filled by up to 877 m of late Paleozoic and Cenozoic strata (Andreis et al., 1986), thus, the true profile of the paleovalley cannot be observed as the current U shape is cut on the top of the preserved Paleozoic fill. The hypothesis that the surrounding ranges experienced alpine glaciation in the mid-Carboniferous and preserve a glacial geomorphic expression (Sterren and Martínez, 1996; Socha et al., 2014) is also not warranted as the tributary paleovalleys in the Sierra de Malanzán and Sierra de Chepes ranges do not show the steep headwalls of cirques that are characteristic of glaciated mountain ranges. The topography in these ranges exhibit structurally-controlled fluvial erosion patterns rather than that of a glacially carved landscape.

Concerning the Olta-Malanzán paleovalley as a conduit for an outlet glacier draining an eastern ice sheet, this concept is untenable as the variable width of the valley is inconsistent with such an interpretation. Outlet glaciers typically are of uniform width of several to tens of km wide (see *Google Earth* images of Antarctic outlet glaciers), and they typically increase in width "downstream" of confluences where tributary glaciers provide an increase in ice volume resulting in greater down-valley erosion. The Olta-Malanzán paleovalley is ~0.5 km wide at its eastern end, narrows to less than 0.2 km wide in its central portion and then is over 5.5 km wide at its western end. The narrowest portions of the paleovalley actually occur in the central portion of the paleovalley where a tributary paleovalley enters the trunk valley. This area, which displays near vertical granitic valley walls, is less than 0.2 km wide (Figs. 2 and 5). Such an arrangement is inconsistent with an interpretation of the paleovalley as carved by an outlet glacier.

Exposures of the paleovalley wall directly in contact with the Malanzán Fm. were observed to be jagged and uneven, with thin slabs of schist projecting into overlying strata, or to be a planar, non-polished, and non-striated surface cut on granite. This contrasts with comparatively smooth or polished surfaces observed on glacially abraded floors and walls of paleovalleys in the present Precordillera region (Colombo et al., 2014; Aquino et al., 2014). Socha et al. (2014) suggested that the absence of these features on bedrock surfaces and on clasts was due to intense weathering as they used heavily weathered granite clasts in the western parts of the Olta paleovalley to emphasize their point. However, the weathered conglomerate clasts that they observed were not in the Malanzán Fm., but were in the Solca Fm., which is late Carboniferous to Permian in age (Net and Limarino, 1999; Gulbranson et al., 2010). The only other reported basement-Malanzán contact (Socha et al., 2014) occurs at section OV9. However, examination reveals that the alleged exposure is actually a granite clast 9 m in diameter.

Andreis et al. (1986) consider the Malanzán paleovalley to have formed as a narrow graben oriented perpendicular to the axis of the uplifted basement block. Net and Limarino (1999) suggested that the location and orientation of the Olta and Malanzán paleovalleys were controlled by a major northwest-southeast trending lineament and that the paleovalley experienced high rates of subsidence relative to the surrounding ranges during early stages of deposition. The Olta-Malanzán paleovalley displays a "lazy-S" shape in plan view (Fig. 2), which is typical of pull-apart basins formed by strike-slip movements (Mann et al., 1983; Hempton and Dunne, 1984). Although our work does little to contribute to an understanding of a tectonic origin, we found no evidence to suggest that the paleovalley was glacially carved.

3.1. Depositional setting

Socha et al. (2014) interpreted poorly sorted, boulder-rich deposits in the Olta paleovalley as basal tillites, and suggested that deformed conglomerates and lake deposits were the result of either subglacial deformation or glacial shove. They also interpreted the thick successions of sandy conglomerate and diamictite (Facies A and B) in the central portion of the valley as a moraine. However, we offer a different non-glacial interpretation for the origin of these sediments (Fig. 16). We interpret the conglomerates and diamictites as alluvial fan/fan delta deposits based on their: (1) bedded nature; (2) wedge-shaped geometries; (3) lateral changes in clast size; (4) downlapping and interfingering nature with sandstones (Facies D) in the direction of paleoflow; (5) predominantly sharp, non-erosive lower contacts and normally-graded upper contacts; (6) local clast lithologies; (7) lack of glacial abrasion features; and (8) lack of mud in the interstitial spaces between clasts (except in a few places where diamictite lenses interfinger with the bedded conglomerates and sandstones). Likewise, features in the folded beds that are inconsistent with subglacial deformation or glacial shove include: (1) a lack of glacial abrasion features; (2) an absence of horizontal/sub-horizontal shear structures; (3) the occurrence of gravel load and pseudonodule structures; (4) the occurrence of flame structures; (5) the reoccurring pattern of alternating load and flame structures along the length of the outcrop; (6) the occurrence of load and flame structures within thick, wave-rippled, sandstone successions; and (7) the occurrence of circular diapiric structures (ruck structures; cf. Thomas and Connell, 1985) surrounding m-scale clast. Soft-sediment deformational structures, which include loads, pseudonodule and flame structures, form due to substrate failure during liquefaction. Liquefaction triggers include: seismic activity, storms, landslides, and rock fall, all of which could have occurred in the Olta paleovalley (cf. Shanmugam, 2016). Because ruck structures are associated with m-scale boulders that deform sandstone and mudstone in the narrowest part of the paleovalley, we interpret these structures to have resulted from rock fall off the steep valley walls, which resulted in clast being dropped onto soft, shallow, lake sediments (Figs. 9, 14 and 16).

In regards to the fill of the paleovalley, Malanzán sedimentation began with high-volume stream and debris flows events (Facies A and B; Figs. 8 and 16) in the steep, narrow, paleo-tributary valleys that then formed alluvial fans/fan deltas that prograded across the narrow, central portion of the main Olta paleovalley. Progradation of the alluvial fans/fan deltas are indicated by an increase in boulder conglomerates upward within the succession, and the downlapping and interfingering of conglomerate beds onto underlying shallow-water sandstones. Such deposition impounded drainage and promoted lake development to the east of these obstructions (Facies D, F, and G; cf. Colombo et al., 2009, Figs. 4 and 16). Mass movement and sediment gravity flows also occurred and contributed to blocking drainage in the paleovalley. These processes included: (1) rockfalls off steep valley walls as represented by boulder breccias (Facies C) and ruck structures surrounding m-scale boulders (Facies H); (2) debris flows as indicated by clast-rich sandy diamictites with clast-supported flow snouts and floating boulders (Facies A); and (3) high and low density turbidity currents as indicated by graded-sandstone and pebbly sandstone beds (Facies D; Fig. 16).

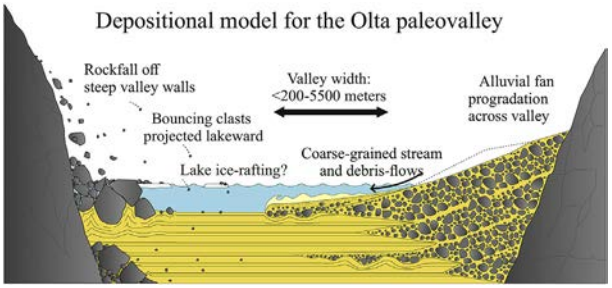

Fig. 16. Model for deposition in the Malanzán Formation in the Olta paleovalley.

Lake sediments, represented by high- and low-density turbidites/hyperpycnites (Facies D), interfinger with fan conglomerates within the main paleovalley, suggesting that a series of alluvial fans/fan deltas and rock falls impounded water bodies in the eastern portion of the paleovalley system (Fig. 16). This is consistent with interpretations for the initiation of lake development in the neighboring Malanzán paleovalley by Andreis et al. (1986).

In the eastern end of the Olta paleovalley, a fining-upwards succession exhibits a transition from proximal to distal turbidites/hyperpycnites, which likely represents progressive deepening of the lake due to progressive blockage of the valley by prograding alluvial fans and developing fan deltas. However, the lake likely stayed shallow through most of this early stage, as evidenced by the occurrence of symmetrical ripples throughout the middle portion of the eastern sections. Evidence of a deeper lake phase or a marine transgression from the west is recorded in the western part of the Olta paleovalley, where a fining upward succession near the top of the Malanzán Fm. shows subaerial/shallow water deposits (Facies E) overlain by interbedded mudstones and very fine-grained sandstones deposited by either storm beds or distal underflow deposits. These, in turn, are overlain by thick laminated mudstones deposited from suspension (Facies F). At its deepest, the lake was at least 40 m deep, as evidenced by the thickness of foreset beds contained in the Gilbert-type delta deposits. However, uppermost foreset or topset beds were not preserved (Facies I).

The outsized clasts present throughout the fine-grained members of the Malanzán Fm. have been interpreted as dropstones, and are the primary lines of evidence that some authors use to suggest a glaciolacustrine or glacially-influence marine setting for this unit (Buatois and Mángano, 1995; Sterren and Martínez, 1996; Net and Limarino, 1999). However, no study to date has reported evidence of glacial abrasion for the clasts. Although Sterren and Martínez (1996) alluded to the presence of exotic clast lithologies, no other study, including this study, have recognized such clasts in the Malanzán Fm. Andreis and Bossi (1981) and Andreis et al. (1986) reported a non-glacial cold climate for the Malanzán Fm. in the Malanzán portion of the paleovalley based on the absence of glacial features, cold and humid paleobotanical assemblages and fan types, and the wide distribution of outsized clasts throughout the formation, which they suggest was evidence for a seasonally-frozen lake surface. We concur with their interpretation for the Olta portion of the paleovalley. We found extensive evidence of mass transport off the steep paleovalley walls into the lake, and the occurrence of high-gradient tributary streams that deposited coarse-grained material in distal portions of the alluvial fan/fan deltas. Deposition of this type during cold months would have occurred onto lake/sea ice, and the clasts would have subsequently been rafted on top of the surface ice as it broke up and drifted across the lake or marine embayment. Rock fall and bouncing clast off walls within a narrow paleovalley would also produce dropstones and ruck structures (Figs. 14 and 16). Rafting of outsized clast by anchor ice or vegetation could have also occurred.

While the fine-grained facies in the Malanzán Fm. were traditionally interpreted as lacustrine (Bracaccini, 1948; Andreis et al., 1986; Limarino and Césari, 1988; Buatois et al., 1994; Buatois and Mángano, 1995; Sterren and Martínez, 1996), the occurrence of brackish water fossil acritarchs and algal species suggest a marine connection (Gutiérrez and Limarino, 2001; Limarino et al., 2002, 2006; Pérez Loinaze, 2009), which correlates with early Pennsylvanian postglacial transgressive marine deposits of the Guandacol, Jejenes, and Lagares formations in the western Paganzo basin (Net et al., 2002; Pazos, 2002; Kneller et al., 2004; Dykstra et al., 2006). While no evidence directly supporting or contradicting this interpretation was identified in this study, the suggestion that the Olta paleovalley was at sea level in the mid-Carboniferous is in contrast to previous ideas for its setting as a mountain valley located at some distance from the Panthalassan Ocean (cf. Andreis et al., 1986; Buatois and Mángano, 1995). Late stages of deposition within the Malanzán Fm. exposed above the study interval and also outside of the study area record a shift from fluvio-deltaic deposition to braided-fluvial sedimentation of the Loma Larga Fm. followed by continued filling of the paleovalley throughout the latest Carboniferous and early Permian as evidenced by predominantly fluvial red-bed conglomerates and sandstones of the Solca, Arroyo Totoral, and La Colina formations, which show increasing aridification into the Permian (Andreis et al., 1986; Net and Limarino, 1999; Gulbranson et al., 2010; Pauls et al., 2017).

3.2. Implications for mid-carboniferous ice volume in the eastern Paganzo basin

Although conditions favoring glacial formation during the LPIA occurred in the Precordillera region (Protoprecordillera/Tontal Arch), along the western margin of the Paganzo Basin, and farther east in the Paraná, Sauce Grande and Chaco Paraná basins, the absence of glacial indicators in the Olta paleovalley suggests that conditions on the eastern-most side of the Paganzo Basin were unfavorable for glacial formation. Factors that limit the accumulation of ice in time and space may include: (1) insolation controlled by orbital parameters, (2) changing paleogeographical positions, (3) changes in atmospheric CO_2 levels, (4) an absence of substantial elevation for ice accumulation, and/or (5) an absence of a substantial moisture source. As stated earlier, deglaciation in western Argentina began during the Early Pennsylvanian (Bashkirian) while ice continued to be supplied to South American basins at the same paleolatitude farther to the east. Such a climate paradox is difficult to explain using global climate drivers such as orbital parameters, changing levels of atmospheric CO_2, or even drift of Gondwana across the South Pole. Global drivers would likely have resulted in near synchronous deglaciation for a given latitude, but would not have resulted in deglaciation in one area while glaciation continued in adjacent areas at the same paleolatitude. To explain such an asynchronous climate in central South America, local controls acting over millions of years (e.g., time between glacial cycles), such as tectonics and changing paleogeographic conditions need to be considered.

The Equilibrium Line Altitude (ELA) is a hypothetical surface that defines the elevation above which glaciers form with respect to latitude with net accumulation of ice occurring above the ELA and net ablation below this surface. The ELA is at or near sea level in the Polar Regions and rises towards the equator where the surface may reside at elevations of over 5000 m (Sugden and John, 1976; Broecker and Denton, 1990). Temporally, the elevation of the surface rises during times of glacial minima, due to elevated mean global temperatures, and falls due to cooling during glacial periods. Aquino et al. (2014) and Valdez-Buso et al. (2017) suggested that the paleovalleys in Argentina were ~2 km deep. However, the combination of thermochronometric data and identification of the paleovalley floor at sea level suggest that the range containing the Olta- Malanzán paleovalley may have been as much as 4000 m high (Enkelmann et al., 2014). Plate reconstructions place western Argentina between 40 and 65° S in the Bashkirian (Powell and Li, 1994; Isbell et al., 2012; Lawver et al., 2011; Torsvik and Cocks, 2013), which corresponds to an ELA between 2000 and 4000 m when

compared to the present northern Hemisphere and between 1100 and 3000 m during the Pleistocene (last glacial maximum; cf. Broecker and Denton, 1990). The present northern hemisphere contains a more continuous equator to pole land mass than the southern hemisphere, which makes it more applicable to Gondwana. Such a comparison suggests that the eastern Paganzo mountain range was located at or near the ELA. However, precipitation also plays a role in the elevation of the ELA (cf. Sugden and John, 1976) and determines accumulation rates as precipitation is transformed into ice. The higher the precipitation the lower the ELA, whereas low precipitation rates raise the ELA. Therefore, an absence of moisture due to the development of a rain shadow may have inhibited glaciers from forming in the eastern Paganzo Basin much like the modern Andes serves as a rain shadow for much of western Argentina. Therefore, uplands in the Precordillera area may have served as a moisture barrier between inland areas and the Panthalassan Ocean during the Late Mississippian and Early Pennsylvanian, thus limiting the potential for ice accumulation to the east (Isbell et al., 2012; Limarino et al., 2014). During deposition of the Malanzán Fm., a number of authors have hypothesized that part of the Paganzo Basin was occupied by a lake or that a marine embayment may have extended into the area (Limarino and Césari, 1988; Buatois et al., 1994; Buatois and Mángano, 1995; Sterren and Martínez, 1996). However, the lake/marine embayment may not have been a sufficient source of moisture for glaciation. The occurrence of red beds and eolian deposits in the strata overlying the Malanzán Fm. (Loma Larga, Solca and La Colina formations) within the study area, attest to progressive aridification of the Paganzo Basin throughout the rest of the Paleozoic (Limarino et al., 2002, 2006; 2014; Gulbranson et al., 2010; Pauls et al., 2017). Except for lower elevations in the hinterland, modern marine embayments in southern Chile, the Andes, and proglacial lakes in Santa Cruz Province (Argentina) provide a modern arid hinterland as an analog for the Paganzo basin during the LPIA.

Following accretion of Chilenia to southwestern Gondwana, a westward shift in the position of subduction occurred during the mid-Carboniferous (cf. Ramos, 1988; Limarino et al., 2002, 2006; Astini et al., 2009; Astini, 2010). Although the tectonic configuration of the Paganzo Basin during glacial time and the importance of the Precordillera region as an upland is in dispute (cf. Limarino et al., 2002, 2006; Astini, 2010; Valdez Buso et al., 2017), the occurrence of paleovalleys > 1000 m deep and the segregation of varying detrital compositions (e.g., sandstone detrital modes and composition of gravel-sized clasts) on different sides of the proposed highland attest to the occurrence of extensive relief along the western side of the Paganzo Basin, which allowed for an early Bashkirian glaciated landscape (cf., López-Gamundí et al., 1994; Limarino et al., 2002, 2006, 2014; Net and Limarino, 2006; Kneller et al., 2004; Dykstra et al., 2006; Henry et al., 2008; Aquino et al., 2014, Valdez Buso et al., 2017). However, later Pennsylvanian and Early Permian breaching and collapse of this range is suggested by several lines of evidence, which include: (1) onlap of postglacial marine strata onto the walls and final overtopping of the paleovalleys in the Precordillera region indicating subsidence of the former upland, (2) expansion of the Paganzo Basin due to back-arc extension indicating changing tectonic conditions, and (3) the common occurrence of sandstone compositions in basins on opposite sides of the former structure indicating that the mountains no longer served as a barrier to sediment dispersal systems (López-Gamundí et al., 1994; Limarino et al., 2002, 2006; 2014; Net and Limarino, 2006; Henry et al., 2008, 2010; Gulbranson et al., 2010; Tedesco et al., 2010; Isbell et al., 2012). With such a collapse, subsidence of the land surface below the ELA would have prevented continued glaciation in western Argentina. Additionally, the changing tectonic conditions resulted in the westward shift in the position of the active margin and development of a volcanic arc along the reconfigured margin. Such a change would have produced a westward shift in the position of the rain shadow, and a resultant westward expansion of an arid climatic zone in western Argentina. Although the uplands that fed ice into the Paraná, Sauce Grande, and Chaco-Paraná basins farther to the east are not fully understood, the occurrence of an inland seaway and substantial elevations in western Africa could have provided for the moisture and the elevation necessary to sustain ice centers there long after ice in western Argentina had disappeared (Rocha Campos et al., 2008; Isbell et al., 2012; Limarino et al., 2014).

4. Conclusions

The sedimentology of the Malanzán Fm. in the Olta paleovalley suggests non-glacial deposition in the mid-Carboniferous. Lake environments developed in the eastern part of the paleovalley as drainage was impounded by the progradation of coarse-grained alluvial fans and fan deltas across a narrow mountain valley. A transgressive lacustrine event is recorded by a fining-upwards succession from sandstones to laminated mudstones in the eastern part of the paleovalley, while western portions record a potential marine transgression and a later transition to fluvio-deltaic deposition. Rock avalanches occurred off the steep valley walls and stream and debris flows deposited coarse clastics on fan/fan deltas that prograded into the lake deforming the soft lake sediment. Prominent soft sediment deformation horizons in the form of load, pseudonodule, and flame structures resulted from liquefaction that may have been triggered by seismic activity, landslides, or major rock fall events. Outsized pebbles and cobbles within both shallow-water sandstones and deeper-water mudstones indicate rafting by lake ice, anchor ice, vegetation, projection of clasts during rockfalls, and/or as out-runner clasts carried by turbidity currents. No obvious glacial signature was found within the facies, clasts, bedrock surfaces, or geomorphology of the valley.

The eastern Paganzo Basin is anomalous as it occurred between two glaciated areas that occupied a similar paleolatitude; basins in western Argentina (western Paganzo, Calingasta-Uspallata, and Rio Blanco basins) and basins in east central South America (Paraná, Chaco-Paraná, and Sauce Grande). Furthermore, western Argentina experienced deglaciation during the Early Pennsylvanian while eastern South America became ice free in the latest Pennsylvanian and Early Permian. This disparity cannot be explained using global climate drivers. However, shifting tectonics conditions including a westward shift in the position of the active margin and tectonically driven uplifts, a westward expansion of the area influenced by a rain shadow, collapse of uplifts in the Precordillera region, and a lack of a sufficient moisture source may have all played a role in inhibiting glaciers in the eastern Paganzo Basin and the early demise of glaciers in uplifts adjacent to the western portions of the same basin.

Acknowledgements

Financial support from this study was provided by the Geological Society of America, the Society for Sedimentary Geologists, the University of Wisconsin-Milwaukee Center for Latin American and Caribbean studies, the Wisconsin Geological Society, a UWM RGI grant, the UWM Department of Geosciences, the Universidad de Buenos Aires, CONICET, and grants from the USA National Science Foundation (Grants 1443557, 1559231, and 1729219).

Appendix A. Supplementary data

Supplementary data related to this article can be found at http://dx.doi.org/10.1016/j.jsames.2018.03.015.

References

Alfaro, P., Gibert, L., Moretti, M., Garcia-Tortosa, F.J., Sanz de Galdeano, C., Galindo-Zaldivar, J., Lopez-Garrido, A.C., 2010. The Significance of Giant Seismites in the Plio-pleistocene Baza Palaeo-lake (S Spain), vol. 22. Terra Nova, pp. 172–179.
Andreis, R.R., Bossi, G.E., 1981. Algunos ciclos lacustres en la Formación Malanzán (Carbónico superior) en la región de Malanzán, sierra de Los Llanos, provincia de La

Rioja. In: Publicado en: 8o. Congreso Geológico Argentino, vol. 4. Actas, San Luis, pp. 639–655.
Andreis, R.R., Cúneo, R., Rolón, A.D., 1985. Definición formal de los "Estratos de Arroyo Totoral" Pérmico inferior, Sierra de Los Llanos, Provincia de La Rioja. In: Actas del Congreso Geológico Argentino, vol. 9. pp. 209–229.
Andreis, R.R., Leguizamón, R., Archangelsky, S., 1986. El paleovalle de Malanzán; nuevos criterios para la estratigrafia del Neopaleozoico de la Sierra de Los Llanos, La Rioja, República Argentina. Bol. Acad. Nac. Cien. 57, 3–119.
Aquino, C.D., Milana, J.P., Faccini, U.F., 2014. New glacial evidences at the Talacasto paleofjord (Paganzo basin, W-Argentina) and its implications for the paleogeography of the Gondwana margin. J. S. Am. Earth Sci. 56, 278–300.
Astini, R., 2010. Linked basins and sedimentary products across an accretionary margin: the case for the late history of the peri-Gondwanan Terra Australis orogen through the stratigraphic record of the Paganzo Basin. In: Papa, C., Astini, R. (Eds.), Field Excursion Guidebook, 18th International Sedimentological Congress. International Association of Sedimentologists, Mendoza, Argentina, pp. 58.
Astini, R.A., Martina, F., Ezpeleta, M., Dávila, F.D., Cawood, P.A., 2009. Chronology from Rifting to Foreland Basin in the Paganzo Basin (Argentina), and a Reapprisal on the "eo- and Neohercynian" Tectonics along Western Gondwana., XII Congreso Geológico Chileno, Santiago, Chile. Universidad de Chile, Santiago, Chile, pp. 1–4 Extended Abstracts S9 010.
Azcuy, C.A., 1975. Miosporas sel Namuriano y Westfaliano de la comarca de Malanzán-Loma Larga, provincia de La Rioja, Argentina. II, vol. 12. Descripciones sistemáticas y significado estratigráfico de las microfloras, Ameghiniana, pp. 113–163.
Azcuy, C.L., Andreis, R.R., Cuerda, A., Hünicken, M.A., Pensa, M.V., Valencio, D.A., Vilas, J.F., Amos, A.J., Archangelsky, S., Berkowski, D.A., Leguizamón, R., 1987. Cuenca Paganzo. In: Archangelsky, S., Amos, A.J., Andreis, R., Azcuy, C.L., González, C.R., López-Gamundí, O., Sabattini, N. (Eds.), El sistema Carbonífero en la República Argentina. Academia Nacional De Ciencias, Córdoba, pp. 41–100.
Balseiro, D., Rustán, J.J., Ezpeleta, M., Vaccari, N.E., 2009. A new Serpukhovian (Mississippian) fossil flora from western Argentina: paleoclimatic, paleobiogeographic and stratigraphic implications. Palaeogeogr. Palaeoclimatol. Palaeoecol. 280, 517–531.
Bennett, M.R., Doyle, P., Mather, A.E., Woodfin, J.L., 1994. Testing the climatic significance of dropstones: an example from southeast Spain. Geol. Mag. 131, 845–848.
Best, J.L., Ashworth, P.J., Bristow, C.S., Roden, J., 2003. Three-dimensional sedimentary architecture of a large, mid-channel sand braid bar, Jamuna river, Bangladesh. J. Sediment. Res. 73, 516–530.
Blair, T.C., 1987. Sedimentary processes, vertical stratification sequences, and geomorphology of the Roaring River alluvial fan, Rocky Mountain National Park, Colorado. J. Sediment. Petrol. 57 (1), 1–18.
Blair, T.C., 2001. Outburst Flood Sedimentation on the Proglacial Tuttle Canyon Alluvial Fan, Owens Valley, California, U.S.A. J. Sediment. Res. 71 (5), 657–679.
Blair, T.C., McPherson, J.G., 1994. Alluvial fans and their natural distinction from rivers based on morphology, hydraulic processes, sedimentary processes, and facies assemblages. J. Sediment. Res. B Stratigr. Global Stud. 64, 450–489.
Boulton, G.S., 1990. Sedimentary and sea level changes during glacial cycles and their control on glacimarine facies architecture. In: In: Dowdeswell, J.A., Scourse, J.D. (Eds.), Glaciomarine Environments: Processes and Sediments, vol. 53. Geological Society of London, Special Publications, pp. 15–52.
Bouma, A.H., 1962. Sedimentology of Some Flysch Deposits; a Graphic Approach to Facies Interpretation. Elsevier, Amsterdam/New York.
Bracaccini, I.O., 1948. Los Estratos de Paganzo y sus niveles plantíferos en la Sierra de los Llanos (provincial de La Rioja). Rev. Asoc. Geol. Argent. 1, 19–61.
Bridge, J.S., Lunt, I.A., 2006. Depositional models of braided rivers. Special Publ. Int. Assoc. Sedimentol. 36, 11–50.
Broecker, W.S., Denton, G.H., 1990. What drives glacial cycles? Sci. Am. 262, 49–56.
Buatois, L.A., Limarino, C.O., Césari, S., 1994. Carboniferous lacustrine deposits from the Palanzo Basin, Argentina. In: Gierlowski-Kordesch, E., Kelts, K. (Eds.), Global Geological Record of Lake Basins. Cambridge University Press, Cambridge, Cambridge, United Kingdom, pp. 135–140.
Buatois, L.A., Mángano, M.G., 1994. Lithofacies and depositional processes from a Carboniferous lake, Sierra de Narvaez, Northwest Argentina. Sediment. Geol. 93, 25–49.
Buatois, L.A., Mángano, M.G., 1995. Post glacial lacustrine event sedimentation in an ancient mountain setting: Carboniferous Lake Malanzán (western Argentina). J. Paleolimnol. 14, 1–22.
Cagliari, J., Philipp, R.P., Buso, V.V., Netto, R.G., Klaus Hillebrand, P., da Cunha Lopes, R., Stipp Basei, M.A., Faccini, U.F., 2016. Age constraints of the glaciation in the Parana Basin; evidence from new U-Pb dates. J. Geol. Soc. Lond. 173, 871–874.
Caputo, M.V., Crowell, J.C., 1985. Migration of glacial centers across Gondwana during Paleozoic Era. Geol. Soc. Am. Bull. 96, 1020–1036.
Caputo, M.V., de Melo, J.H.G., Streel, M., Isbell, J.L., 2008. Late Devonian and Early Carboniferous glacial records of South America. In: Fielding, C.R., Frank, T.D., Isbell, J.L. (Eds.), Resolving the Late Paleozoic Ice Age in Time and Space. Geological Society of America Special Publication, Boulder, CO, pp. 161–173.
Carignano, C., Cioccale, M., Rabassa, J., 1999. Landscape antiquity of the central-eastern Sierras Pampeanas (Argentina); geomorphological evolution since Gondwanic times. Zeitschrift fuer Geomorphologie. Supplementband 118, 245–268.
Carto, S.L., Eyles, N., 2012. Sedimentology of the Neoproterozoic (c. 580 Ma) Squantum 'Tillite', Boston Basin, USA: Mass flow deposition in a deep-water arc basin lacking direct glacial influence. Sediment. Geol. 269–270, 1–14.
Catuneanu, O., 2006. Principles of Sequence Stratigraphy. Elsevier Science, Amsterdam.
Césari, S.N., Limarino, C.O., Gulbranson, E.L., 2011. An Upper Paleozoic bio-chronostratigraphic scheme for the western margin of Gondwana. Earth Sci. Rev. 106, 149–160.
Colella, A., De Boer, P.L., Nio, S.D., 1987. Sedimentology of a marine intermontane Pleistocene Gilbert-type fan-delta complex in the Crati Basin, Calabria, southern Italy. Sedimentology 34, 721–736.
Colombo, F., Busquets, P., Porta, N.S.d., Limarino, C.O., Heredia, N., Rodríguez-Fernández, L.R., Alvarez-Marron, J., 2009. Holocene intramontane lake development: A new model in the Jáchal River Valley, Andean Precordillera, San Juan, Argentina. J. S. Am. Earth Sci. 28, 229–238.
Colombo, F., Limarino, C.O., Spalletti, L.A., Busquets, P., Cardó, R., Méndez-Bedia, I., Heredia, N., 2014. Late Palaeozoic lithostratigraphy of the Andean Precordillera revisited (San Juan Province, Argentina). J. Iber. Geol. 40, 241–259.
Crookshanks, S., Gilbert, R., 2008. Continuous, diurnally fluctuating turbidity currents in Kluane Lake, Yukon Territory. Can. J. Earth Sci. 45, 1123–1138.
Dadson, S., Hovius, N., Pegg, S., Dade, W.B., Horng, M.J., Chen, H., 2005. Hyperpycnal river flows from an active mountain belt. J. Geophys. Res. 110, 04–16.
Dionne, J.-C., 1993. Sediment load of shore ice and ice rafting potential, upper St. Lawrence Estuary, Quebec, Canada. J. Coast Res. 9, 628–646.
Dykstra, M., Kneller, B., Milana, J.P., 2006. Deglacial and postglacial sedimentary architecture in a deeply incised paleovalley–paleofjord — the Pennsylvanian (late Carboniferous) Jejenes Formation, San Juan, Argentina. Geol. Soc. Am. Bull. 118, 913–937.
Enkelmann, E., Ridgway, K.D., Carignano, C., Linnemann, U., 2014. A thermochronometric view into an ancient landscape: tectonic setting, development, and inversion of the Paleozoic eastern Paganzo basin, Argentina. Lithosphere 6, 93–107.
Fielding, C.R., Frank, T.D., Birgenheier, L.P., Rygel, M.C., Jones, A.T., Roberts, J., 2008a. Stratigraphic imprint of the Late Paleozoic Ice Age in eastern Australia: a record of alternating glacial and nonglacial climate regime. J. Geol. Soc. Lond. 165, 129–140.
Fielding, C.R., Frank, T.D., Birgenheier, L.P., Rygel, M.C., Jones, A.T., Roberts, J., 2008b. Stratigraphic record and facies associations of the late Paleozoic ice age in eastern Australia (New South Wales and Queensland). In: Fielding, C.R., Frank, T., Isbell, J.L. (Eds.), Resolving the Late Paleozoic Ice Age in Time and Space. Geological Society of America, pp. 41–57 Special Paper 441.
Fielding, C.R., Frank, T.D., Isbell, J.L., 2008c. The late Paleozoic ice age–A review of current understanding and synthesis of global climate patterns. In: Fielding, C.R., Frank, T.D., Isbell, J.L. (Eds.), Resolving the Late Paleozoic Ice Age in Time and Space. Geological Society of America, pp. 343–354 Special Paper 441.
Frank, T.D., Shultis, A.I., Fielding, C.R., 2015. Acme and demise of the late Palaeozoic ice age: A view from the southeastern margin of Gondwana. Palaeogeogr. Palaeoclimatol. Palaeoecol. 418, 176–192.
Galloway, W.E., 1989. Genetic stratigraphic sequences in basin analysis; I, Architecture and genesis of flooding-surface bounded depositional units. AAPG (Am. Assoc. Pet. Geol.) Bull. 73, 125–142.
Gilbert, R., 1990. Rafting in glacimarine environments. In: In: Dowdeswell, J.A., Scourse, J.D. (Eds.), Glacimarine Environments: Processes and Sediments, vol. 53. Geological Society London Special Publications, pp. 105–120.
Girardclos, S., Schmidt, O.T., Sturm, M., Ariztegui, D., Pugin, A., Anselmetti, F.S., 2007. The 1996 AD delta collapse and large turbidite in Lake Brienz. Mar. Geol. 241, 137–154.
Godt, J.W., Coe, J.A., 2007. Alpine debris flows triggered by a 28 July 1999 thunderstorm in the central Front Range, Colorado. Geomorphology 84, 80–97.
Griffis, N.P., Mundil, R., Montañez, I.P., Isbell, J.L., Fedorchuk, N., Vesely, F., Iannuzzi, R., Yin, Q.Z., 2017. A new stratigraphic framework built on U-Pb single-zircon TIMS ages and implications for the timing of the penultimate icehouse (Paraná Basin, Brazil). Geol. Assoc. Am. Bull. https://doi.org/10.1130/B31775.1.
Gulbranson, E.L., Montañez, I.P., Schmitz, M.D., Limarino, C.O., Isbell, J.L., Marenssi, S.A., Crowley, J.L., 2010. High-precision U–Pb calibration of Carboniferous glaciation and climate history, Paganzo Group, NW Argentina. GSA Bull. 122, 1480–1498.
Gulbranson, E.L., Montañez, I.P., Tabor, N., Limarino, C.O., 2015. Late Pennsylvanian aridification on the southwestern margin of Gondwana (Paganzo Basin, NW Argentina): A regional expression of a global climate perturbation. Palaeogeogr. Palaeoclimatol. Palaeoecol. 417, 220–235.
Gutiérrez, P.R., Limarino, C.O., 2001. Palinología de la Formación Malanzán (Carbonifero Superior), La Rioja, Argentina, vol. 38. Nuevos datos y consideraciones paleoambientales, Ameghiniana, pp. 99–118.
Hambrey, M.J., Glasser, N.F., 2012. Discriminating glacier thermal and dynamic regimes in the sedimentary record. Sediment. Geol. 251–252, 1–33.
Harvey, A.M., 1990. Factors influencing Quaternary alluvial fan development in southeast Spain. In: Rachocki, A.H., Church, M. (Eds.), Alluvial Fans: a Field Approach. Wiley, Chichester, pp. 247–269.
Hempton, M.R., Dunne, L.A., 1984. Sedimentation in pull-apart basins: active examples in eastern Turkey. J. Geol. 92, 513–530.
Henry, L.C., Isbell, J.L., Limarino, C.O., 2008. Carboniferous glacigenic deposits of the Protoprecordillera of west central Argentina. In: Fielding, C.R., Frank, T.D., Isbell, J.L. (Eds.), Resolving the Late Paleozoic Ice Age in Time and Space. Geological Society of America, pp. 131–142 Special Paper, 441.
Henry, L.C., Isbell, J.L., Limarino, C.O., McHenry, L.J., Fraiser, M.L., 2010. Mid-Carboniferous deglaciation of the Protoprecordillera, Argentina recorded in the Agua de Jagüel palaeovalley. Palaeogeogr. Palaeoclimatol. Palaeoecol. 298, 112–129.
Hiscott, R.N., Pickering, K.T., 1984. Reflected turbidity currents on an Ordovician basin floor, Canadian Appalachians. Nature (London) 311, 143–145.
Holz, M., Souza, P.A., Iannuzzi, R., 2008. Sequence stratigraphy and biostratigraphy of the Late Carboniferous to Early Permian glacial succession (Itararé subgroup) at the eastern-southeastern margin of the Paraná Basin, Brazil. In: Fielding, C.R., Frank, T., Isbell, J.L. (Eds.), Resolving the Late Paleozoic Ice Age in Time and Space. Geological Society of America, Boulder, pp. 115–129 Special Paper 441.
Horton, D.E., Poulsen, C.J., 2009. Paradox of late Paleozoic glacioeustacy. Geology 37 (8), 715–718.
Isbell, J.L., Miller, M.F., Wolfe, K.L., Lenaker, P.A., 2003. Timing of late Paleozoic glaciation in Gondwana: was glaciation responsible for the development of northern hemisphere cyclothems? In: Chan, M.A., Archer, A.W. (Eds.), Extreme Depositional Environments: Mega End Members in Geologic Time. Geological Society of America, pp. 5–24 Special Paper 370.
Isbell, J.L., Henry, L.C., Gulbranson, E.L., Limarino, C.O., Fraiser, M.L., Koch, Z.J., Ciccioli, P.L., Dineen, A.A., 2012. Glacial paradoxes during the late Paleozoic ice age: evaluating the equilibrium line altitude as a control on glaciation. Gondwana Res. 22,

1–19.
Jordan, T.E., Zeitler, P., Ramos, V., Gleadow, A.J.W., 1989. Thermochronometric data on the development of the basement peneplain in the Sierras Pampeanas, Argentina. J. S. Am. Earth Sci. 2, 207–222.
Kempema, E.W., Reimnitz, E., Barnes, P.W., 2001. Anchor-ice formation and ice rafting in southwestern Lake Michigan, U.S.A. J. Sediment. Res. 71, 346–354.
Kneller, B., Milana, J.P., Buckee, C., Al Ja'aidi, O.S., 2004. A depositional record of deglaciation in a paleofjord (Late Carboniferous [Pennsylvanian] of San Juan Province, Argentina): the role of catastrophic sedimentation. Geol. Soc. Am. Bull. 116, 348–367.
Lambert, A., Giovanoli, F., 1988. Records of riverborne turbidity currents and indications of slope failures in the Rhone Delta of Lake Geneva. Limnol. Oceanogr. 33, 458–468.
Lawver, L.A., Dalziel, I.W.D., Norton, I.O., Gahagan, L.M., 2011. The Plates 2011 Atlas of Plate Reconstructions (500Ma to Present Day), Plates Progress Report No. 345-0811. University of Texas Technical Report No. 198. University of Texas, Austin, Texas, pp. 189.
Lima, J.H.D., Netto, R.G., 2012. Trace fossils from the Permian Teresina Formation at Cerro Caveiras (S Brazil). Rev. Bras. Palaontol. 15, 5–22.
Limarino, C.O., Césari, S.N., 1988. Paleoclimatic significance of the lacustrine Carboniferous deposits in Northwest Argentina. Palaeogeogr. Palaeoclimatol. Palaeoecol. 65, 115–131.
Limarino, C.O., Césari, S.N., Net, L.I., Marenssi, S.A., Gutiérrez, P.R., Tripaldi, A., 2002. The Upper Carboniferous postglacial transgression in the Paganzo and Río Blanco Basins (northwestern Argentina): facies and stratigraphic significance. J. S. Am. Earth Sci. 15, 445–460.
Limarino, C.O., Césari, S.N., Spalletti, L.A., Taboada, A.C., Isbell, J.L., Geuna, S., Gulbranson, E.L., 2014. A paleoclimatic review of southern South America during the late Paleozoic: a record from icehouse to extreme greenhouse conditions. Gondwana Res. 25, 1396–1421.
Limarino, C., Gutiérrez, P., 1990. Diamictites in the Agua Colorada Formation (northwestern Argentina); new evidence of Carboniferous glaciation in South America. J. S. Am. Earth Sci. 3 (1), 9–20.
Limarino, C.O., Gutiérrez, P., Césari, S.N., 1984. Facies lacustre de la Formaci6n Agua Colorada (Paleozoico superior): aspectos sedimentológicos y contenido paleofloristico. In: Actos IX Congreso Geológico Argentino. 5. pp. 324–341.
Limarino, C.O., Spalletti, L.A., 2006. Paleogeography of the Upper Paleozoic basins of southern South America: an overview. J. S. Am. Earth Sci. 22, 134–155.
Limarino, C.O., Tripaldi, A., Marenssi, S., Fauqué, L., 2006. Tectonic, sea level, and climatic controls on late Paleozoic sedimentation in the western basins of Argentina. J. S. Am. Earth Sci. 33, 205–226.
López-Gamundí, O.R., 1997. Glacial–postglacial transition in the late Paleozoic basins of Southern South America. In: Martini, I.P. (Ed.), Late Glacial and Postglacial Environmental Changes: Quaternary Carboniferous–permian, and Proterozoic. Oxford University Press, Oxford U.K, pp. 147–168.
López-Gamundí, O.R., Espejo, I.S., Conaghan, P.J., Powell, C.McA., Veevers, J.J., 1994. Southern South America. In: In: Veevers, J.J., Powell, C.McA. (Eds.), Permian–triassic Pangean Basins and Foldbelts along the Panthalassan Margin of Gondwanaland, vol. 184. Geological Society of America Memoir, Boulder, Colorado, pp. 281–329.
López-Gamundí, O.R., Martínez, M., 2000. Evidence of glacial abrasion in the Calingasta–Uspallata and western Paganzo Basins, mid-Carboniferous of western Argentina. Palaeogeogr. Palaeoclimatol. Palaeoecol. 159, 145–165.
Mann, P., Hempton, M.R., Bradley, D.C., Burke, K., 1983. Development of pull-apart basins. 1398. J. Geol. 91, 529–554.
Marenssi, S.A., Tripaldi, A., Limarino, C.O., Caselli, A.T., 2005. Facies and architecture of a Carboniferous grounding-line system from the Guandacol Formation, Paganzo Basin, northwestern Argentina. Gondwana Res. 8, 187–202.
Montañez, I.P., Poulsen, C.J., 2013. The late Paleozoic ice age: an evolving paradigm. Annu. Rev. Earth Planet Sci. 41 24.1–24.28.
Mulder, T., Chapron, E., 2011. Flood deposits in continental and marine environments; character and significance. AAPG Stud. Geol. 61, 1–30.
Mulder, T., Alexander, J., 2001. The physical character of subaqueous sedimentary density flows and their deposits. Sedimentology 48, 269–299.
Mutti, E., Davoli, G., Tinterri, R., Zavala, C., 1996. The importance of ancient fluvio-deltaic systems dominated by catastrophic flooding in tectonically active basins. Estratto da Memorie 01, Screnze Geologiche 48, 233–291.
Nemec, W., Steel, R.J., 1984. Alluvial and coastal conglomerates; their significant features and some comments on gravelly mass-flow deposits. Memoir - Can. Soc. Petrol. Geol. 10, 1–31.
Nemec, W., Steel, R.J., 1988. What is a fan delta and how do we recognize it? In: Nemec, W., Steel, R.J. (Eds.), Fan Deltas: Sedimentology and Tectonic Settings. Blackie, Glasgow and London, pp. 2–13.
Net, L.I., Alonso, M.S., Limarino, C.O., 2002. Source rock and environmental control on clay mineral associations, lower section of Paganzo group (Carboniferous), northwest Argentina. Sediment. Geol. 152, 183–199.
Net, L.I., Limarino, C.O., 1999. Paleogeografía y correlación estratigráfica del Paleozoico Tardío de la Sierra de Los Llanos, Provincia de la Rioja, Argentina. Rev. Asoc. Geol. Argent. 54, 229–239.
Net, L.I., Limarino, C.O., 2006. Applying sandstone petrofacies to unravel the Upper Carboniferous evolution of the Paganzo Basin, northwest Argentina. J. S. Am. Earth Sci. 22, 239–254.
Netto, R.G., Balistieri, P.R.M.N., Lavina, E.L.C., Silveira, D.M., 2009. Ichnological signatures of shallow freshwater lakes in the glacial Itarare Group (Mafra Formation, Upper Carboniferous-Lower Permian of Parana Basin, S Brazil). Palaeogeogr. Palaeoclimatol. Palaeoecol. 272, 240–255.
Pauls, K.N., Isbell, J.L., Moxness, L.D., Limarino, C.O., Schencman, L.J., 2017. Late Paleozoic paleoclimatic comparisons of mid-latitude basins in Western Argentina: Controls on early Pennsylvanian deglaciation in Western Gondwana. Geol. Soc. Am. Abstr. Progr. 49, 6,. http://dx.doi.org/10.1130/abs/2017AM-300103.
Pazos, P.J., 2002. The Late Carboniferous glacial to postglacial transition: facies and sequence stratigraphy, western Paganzo Basin, Argentina. Gondwana Res. 5, 467–487.
Pérez Loinaze, V.P., 2009. New palynological data from the Malanzán Formation (Carboniferous), La Rioja Province, Argentina. Ameghiniana 46, 495–512.
Postma, G., Nemec, W., Kleinspehn, K.L., 1988. Large floating clasts in turbidites: a mechanism for their emplacement. Sediment. Geol. 58, 47–61.
Powell, C.M., Li, Z.X., 1994. Reconstruction of the Panthalassan margin of Gondwanaland. In: In: Veevers, J.J., Powell, C.M. (Eds.), Permian-triassic Pangean Basins and Foldbelts along the Panthalassan Margin of Gondwanaland, vol. 184. Geological Society of America Memoir, Boulder, Colorado, pp. 5–9.
Rabassa, J., Carignano, C., Cioccale, M., 2014. A general overview of Gondwana landscpaes in Argentina. In: Rabassa, J., Ollier, C. (Eds.), Gondwana Landscapes in Southern South America: Argentina, Uruguay and southern Brazil. Springer Earth System Science, Dordrecht, Heidelberg, New York, London, pp. 201–245.
Ramos, V.A., 1988. Tectonics of the Late Proterozoic–Early Paleozoic: a collisional history of Southern South America. Episodes 11, 168–174.
Ramos, V., Jordan, T., Allmendinger, R., Kay, S., Cortés, J., Palma, M., 1984. Chilenia: un terreno alóctono en la evolución paleozoica de los Andes Centrales. In: 10° Congr. Geol, vol. 2. Actas, Argentino, pp. 84–106.
Ramos, V., Jordan, T., Allmendinger, R., Mpodozis, C., Kay, S., Cortés, J., Palma, M., 1986. Paleozoic terranes of the central Argentine-Chilean Andes. Tectonics 5, 855–888.
Rocha Campos, A.C., dos Santos, P.R., Canuto, J.R., 2008. Late Paleozoic glacial deposits of Brasil: Paraná Basin. In: Fielding, C.R., Frank, T.D., Isbell, J.L. (Eds.), Resolving the Late Paleozoic Ice Age in Time and Space. Geological Society of America, pp. 97–114 Special Paper 441.
Schatz, E.R., Mángano, M.G., Buatois, L.A., Limarino, C.O., 2011. Life in the late Paleozoic ice age: trace fossils from glacially influenced deposits in a late Carboniferous fjord of western Argentina. J. Paleontol. 85, 502–518.
Shanmugam, G., 2016. The Seismite problem. J. Palaeogeogr. 5, 318–362.
Socha, B.J., Carignano, C., Rabassa, J., Mickelson, D.M., 2014. Gondwana glacial paleolandscape, diamictite record of Carboniferous valley glaciation, and preglacial remnants of an ancient weathering front in northwestern Argentina. In: Rabassa, J., Ollier, C. (Eds.), Gondwana Landscapes in Southern South America. Springer, Dordrecht, pp. 331–363.
Sohn, Y.K., 2000. Depositional processes of submarine debris flows in the Miocene fan deltas, Pohang Basin, SE Korea with special reference to flow transformation. J. Sediment. Res. 70, 491–503.
Stanley, K.O., Surdam, R.C., 1978. Sedimentation on the front of Eocene Gilbert-type deltas, Washakie Basin, Wyoming. J. Sediment. Petrol. 48, 557–573.
Sterren, A.F., Martínez, M., 1996. El paleovalle de Olta (Carbonífero): paleoambientes y paleogeografía. In: 13º Congreso Geológico Argentino y 3º Congreso Exploración de Hidrocarburos (Buenos Aires), vol. 2. Actas, pp. 89–103.
Sugden, D.E., John, B.S., 1976. Glaciers and Landscape: a Geomorphological Approach. Edward Arnold, London.
Syvitski, J.M., Burrell, D.C., Skei, J.M., 1987. Fjords: Processes and Products. Springer-Verlag, New York, pp. 379.
Talling, P.J., 2014. On the triggers, resulting flow types and frequencies of subaqueous sediment density flows in different settings. Mar. Geol. 352, 155–182.
Talling, P.J., Masson, D.G., Sumner, E.J., Malgesini, G., 2012. Subaqueous sediment density flows: Depositional processes and deposit types. Sedimentology 59, 1937–2003.
Tedesco, A., Ciccioli, P., Surian, J., Limarino, C., 2010. Changes in the architecture of fluvial deposits in the Paganzo Basin (Upper Paleozoic of San Juan Province): an example of sea level and climatic controls on the development of coastal fluvial environments. Geol. Acta 8, 463–482.
Thomas, G.S.P., Connell, R.J., 1985. Iceberg drop, dump, and grounding structures from Pleistocene glacio-lacustrine sediments, Scotland. J. Sediment. Petrol. 55 (2), 243–249.
Torsvik, T.H., Cocks, L.R.M., 2013. Gondwana from top to base in space and time. Gondwana Res. 24, 999–1030.
Valdez Buso, V., Pasquo, M.D., Milana, J.P., Kneller, B., Fallgatter, C., Chemale, F.J., Paim, P.S.G., 2017. Integrated U-Pb zircon and palynological/palaeofloristic age determinations of a Bashkirian palaeofjord fill, Quebrada Grande (Western Argentina). J. S. Am. Earth Sci. 73, 202–222.
Van Steijn, H., 1996. Debris-flow magnitude—frequency relationships for mountainous regions of Central and Northwest Europe. Geomorphology 15, 259–273.
Veevers, J.J., Powell, M., 1987. Late Paleozoic glacial episodes in Gondwanaland reflected in transgressive–regressive depositional sequences in Euramerica. Geol. Soc. Am. Bull. 98, 475–487.
Visser, J.N.J., 1983. The problems of recognizing ancient sub- aqueous debris flow deposits in glacial sequences. Trans. Geol. Soc. S. Afr. 86, 127–135.
Woodborne, M.W., Rogers, J., Jarman, N., 1989. The geological significance of kelp-rafted rock along the West Coast of South Africa. Geo Mar. Lett. 9, 109–118.
Zavala, C., Arcuri, M., di Meglio, M., Diaz, H.G., Contreras, C., 2011. A genetic facies tract for the analysis of sustained hyperpycnal flow deposits. AAPG Stud. Geol. 61, 31–51.
Zavala, C., Ponce, J.J., Arcuri, M., Drittanti, D., Freije, H., Asensio, M., 2006. Ancient Lacustrine Hyperpycnites: A Depositional Model from a Case Study in the Rayoso Formation (Cretaceous) of West-Central Argentina. J. Sediment. Res. 76, 41–59.